UAB
Universitat Autònoma
de Barcelona

Bachelor Thesis

Numerical propagation of trajectories of Earth-orbiting spacecraft

Author:
Víctor Ballester

Supervisor:
Josep Maria Mondelo

Bachelor's Degree in Mathematics
Departament de Matemàtiques
Facultat de Ciències

June 26, 2023

We are just an advanced breed of monkeys on a minor planet of a very average star. But we can understand the Universe. That makes us something very special.

Stephen Hawking

Contents

Acknowledgements

I would like to express my gratitude to my supervisor, Josep Maria Mondelo, for his support, invaluable guidance, and extensive expertise throughout the development of this thesis. His constant feedback, attention to detail, and constructive criticism were essential to the completion of this report.

I also want to thank my father for his constant support and revision of the work. His encouragement, critical insights, and our relentless discussions were fundamental in shaping my ideas and approach to the research.

I am also grateful to all the professors who have taught me throughout my course at the university, for their valuable contributions to my education, their passion for their subjects, and their inspiring lectures. Their knowledge, expertise, and dedication made a real impact on my academic growth.

Finally, I would like to acknowledge my colleagues at the university, whose support and enthusiasm have made my academic journey an enjoyable experience. Their friendship, encouragement, and collaboration have been an integral part of my personal and academic development.

Thank you all for your support and guidance.

1 Introduction

The orbital environment of the Earth is very populated. As of mid-2023, there are around 27 500 spacecraft in orbit around the Earth [Spa]. Among these, around 11 000 are active satellites, 2 300 are rocket bodies (that is, the propulsion units used to deploy satellites into orbit), 13 700 are inactive satellites (debris), and the rest are unclassified objects. And, as years go by, the probability of collision between two spacecraft is continuously increasing. Some serious collisions have already taken place, for instance the high-speed collision between the Iridium 33 and the Kosmos-2251 satellites in 2009 [Wikb].

Orbital dynamics around the Earth are very complex. The Keplerian approximation provides accurate results just for a few hours. Important perturbations of the Keplerian approximation are: the actual gravity field of the Earth (non-Keplerian because the Earth is not a point mass nor a sphere with constant density), atmospheric drag, third-body effects (such as the gravitational pull from the Moon and the Sun) and solar radiation pressure. The most accurate models (see [VC08]) include all these perturbations, and are able to make reasonably accurate predictions for a few days. This makes possible to keep a catalog of orbiting objects (both active and inactive) through a heterogeneous global network of observing stations, that can be e.g. optical (telescopes) or radar-based [Spa; Cel]. Keeping this catalog requires continuous observation.

The goal of this work is to give quantitative insight in the effect that these perturbations have individually. For that, the necessary models will be mathematically developed. We will construct a reference frame where the Newton's laws of motion are valid. But since we will have to know the position of the satellites relative to a "fixed" Earth at each step of the integration process, we will have to construct transformations from the former inertial frame to this latter non-inertial frame. In order to do so, we will have to account for the variations on the Earth's axis of rotation as a function of time.

At the end, we will show the results of the simulations for three types of orbits: LEO (Low Earth Orbit), MEO (Medium Earth Orbit) and GEO (Geostationary Earth Orbit).

In this work we have used the software from O. Montenbruck and E. Gill [MG05] for the computation of the geopotential model and most of the transformations between the reference frames explained in Section 3.2.3. Additionally, J. M. Mondelo facilitated me the code for the RK7(8) numerical integrator. Finally, the code for the highly-accurate model that we will use to compare our results, the SGP4 model, was obtained from [Val+][1].

[1] All the code used in this project can be found at https://github.com/victorballester7/final-bachelor-thesis (accessed on June 25, 2023).

2 Conics in a nutshell

In this section we will revise some basic properties of conics, that will be used in the next sections for the study of the motion of two bodies under the influence of gravity.

2.1 General conics

Definition 1. A conic is the curve obtained as the intersection of a plane with the surface of a double cone (a cone with two *nappes*).

In Fig. 1 we show the 3 types of conics: the ellipse, the parabola, and the hyperbola, which differ on their eccentricity, as we will see later on. Note that the circle is a special case of the ellipse. The following

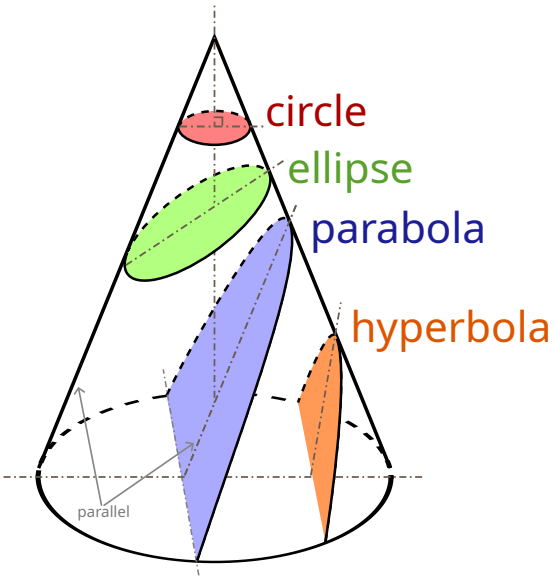

Figure 1: The black boundaries of the colored regions are conic sections. The other half of the hyperbola, which is not shown, is in the other nappe of the double cone. Source: [Mat12].

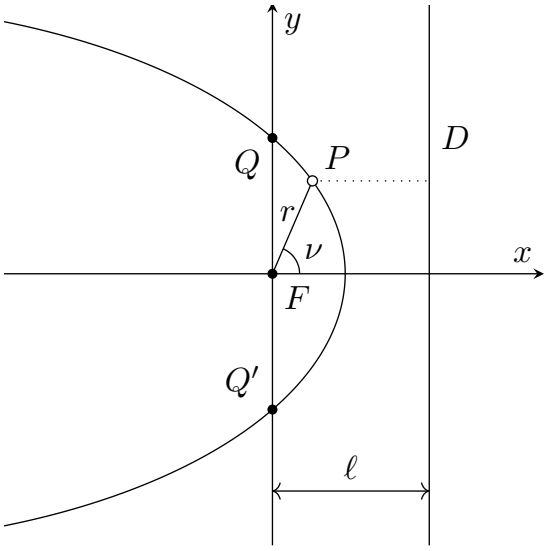

Figure 2: Reference frame centered at the focus of the conic and whose axes are such that the y-axis is parallel to the directrix and the x-axis is perpendicular to the directrix. The directions of the axes are chosen arbitrarily, subject to the constraint that a right-handed system (x, y) is obtained.

proposition gives a characterization of the conics.

Proposition 2. A conic is the set of all points P such that the distance from P to a fixed point F is a multiple of the distance from P to a fixed line D. Mathematically, this is expressed as:

$$d(P, F) = e d(P, D) \tag{1}$$

where d is the Euclidean distance. The point F is called *focus*; the line D, *directrix*, and the constant of proportionality e, *eccentricity*.

An important type of conic section is the case $e = 0$, but this definition is not valid in this case, as it reduces to a single point. In this case, the conic obtained, a *circle*, is defined as the set of all points P such that the distance from P to a fixed point F is constant. It can be thought as a limit case of Eq. (1) by letting the line D approach to infinity at a specific rate.

Note that using the polar coordinates (r, ν) centered at F (as in Fig. 2), we can rewrite Eq. (1) as:

$$r = e(\ell - r\cos\nu) \implies r = \frac{e\ell}{1 + e\cos\nu} =: \frac{p}{1 + e\cos\nu} \tag{2}$$

where we have defined $p := e\ell$.

Definition 3. Let C be a conic and e be its eccentricity. We say that C is

- an *ellipse* if $0 \leq e < 1$.
- a *parabola* if $e = 1$.

- a *hyperbola* if $e > 1$.

If $e = 0$, the conic is called *circle*.

2.2 Ellipse

From now on we will focus on the study of the ellipse. From Eq. (2), since $e < 1$, it follows that $r(\nu)$ is continuous, 2π-periodic and satisfies $r(0) = r(2\pi)$. Therefore, the ellipse is a bounded and closed curve, and it is the only conic section satisfying these two properties.

Let's now study the extrema of $r(\nu)$. An easy check shows that the minimum is attained at $\nu = 0$ and the maximum at $\nu = \pi$ and these values are given by:

$$r_{\min} = \frac{p}{1+e} \qquad \text{and} \qquad r_{\max} = \frac{p}{1-e} \tag{3}$$

When considering orbits of celestial bodies these points are called *periapsis* and *apoapsis*, respectively[2]. The line connecting both points is called *line of apsides*. Let's seek now the extrema of $x = r\cos\nu$ and $y = r\sin\nu$. Differentiating with respect to ν yields:

$$x' = -\frac{p\sin\nu}{(1+e\cos\nu)^2} \qquad y' = \frac{p(e+\cos\nu)}{(1+e\cos\nu)^2} \tag{4}$$

On the one hand, x' vanishes at $\nu = 0, \pi$. Therefore, the extrema of x coincide with the periapsis and apoapsis points and at these points the y coordinate is equal to 0. This means that the line of apsides goes through the focus of the ellipse. On the other hand, y' vanishes at $\cos\nu = -e$. That is, at $\nu = \arccos(-e)$ and $\nu = 2\pi - \arccos(-e)$. Therefore, using that $\sin(\arccos x) = \sqrt{1-x^2}$, the values of y at these extrema are:

$$y_{\min} = \frac{p}{1-e^2}\sin(2\pi - \arccos(-e)) = -\frac{p}{\sqrt{1-e^2}} \qquad y_{\max} = \frac{p}{1-e^2}\sin(\arccos(-e)) = \frac{p}{\sqrt{1-e^2}} \tag{5}$$

Note that the x coordinate at these two points is the same: $-\dfrac{pe}{1-e^2}$.

Definition 4. Consider the reference frame of Fig. 3 centered at one focus. We define the *semi-major axis* a as half the segment that connects the two extrema of the x coordinate. The *semi-minor axis* b is defined as half the segment that connects the two extrema of the y coordinate. The length of those segments are also denoted by a and b, respectively. Thus, these are given by the following expressions:

$$a := \frac{x_{\max} - x_{\min}}{2} = \frac{r_{\max} + r_{\min}}{2} = \frac{p}{1-e^2} \qquad b := \frac{y_{\max} - y_{\min}}{2} = \frac{p}{\sqrt{1-e^2}} \tag{6}$$

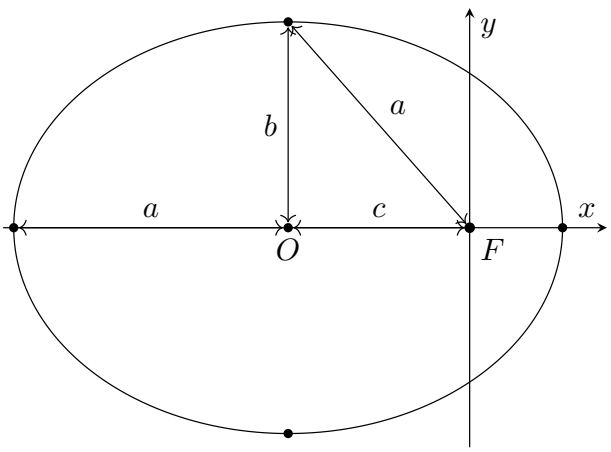

Figure 3: Ellipse

[2]Other names are used in the literature when the central body and the orbiter are particular ones. For example for the system Sun-Earth, the words *perihelion* and *aphelion* are used, whereas for the system Earth-Moon, the words *perigee* and *apogee* are used instead.

From here note that we can express b in terms of a and e as:

$$b = a\sqrt{1-e^2} \tag{7}$$

Definition 5. We define the center of the ellipse O as the intersection of the semi-major axis and semi-minor axis. The *linear eccentricity* c is defined as the distance between the center O and the focus F.

We have just found a relation between a and b. Now, we would like to find a similar relation between a and c. To do so, let's calculate the distance from the focus F to one of the extrema of the y coordinate.

$$d\left(F, \left(-\frac{pe}{1-e^2}, \pm\frac{p}{\sqrt{1-e^2}}\right)\right) = \frac{p}{\sqrt{1-e^2}}\sqrt{\frac{e^2}{1-e^2}+1} = \frac{p}{1-e^2} = a \tag{8}$$

Hence, the value of c can be simplified to (see Fig. 3):

$$c^2 = a^2 - b^2 = a^2 - a^2(1-e^2) = a^2e^2 \implies c = ae \tag{9}$$

Finally, one more property of the ellipse will be needed: its area.

Proposition 6. The area enclosed in an ellipse of semi-major axis a and semi-minor axis b is πab.

Proof. Consider the ellipse E centered at the origin and oriented as in Fig. 4.

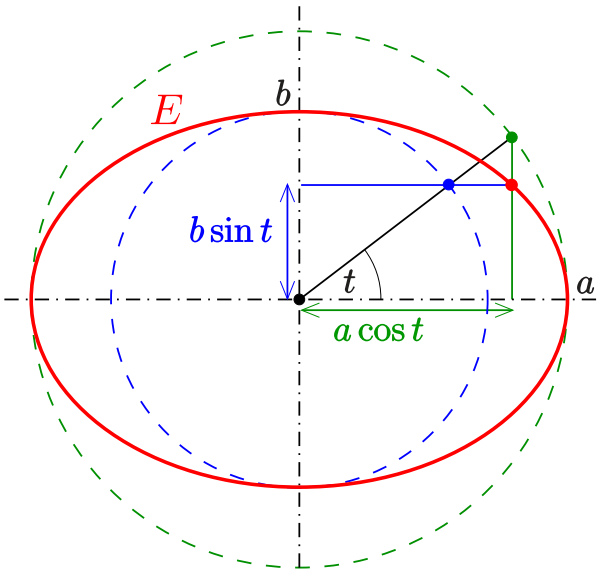

Figure 4: Reference frame centered at the center of the ellipse. Source: [Ag217].

From Fig. 4 one can check that it can be parametrized by $(x, y) = (a\cos t, b\sin t)$ with $t \in [0, 2\pi)$. This parametrization satisfies:

$$\frac{x^2}{a^2} + \frac{y^2}{b^2} = 1 \tag{10}$$

Hence, the area enclosed in the ellipse can be parametrized by $(x, y) = (ar\cos t, br\sin t)$, with $r \in [0, 1]$ and $t \in [0, 2\pi)$. The Jacobian of the transformation $(r, t) \to (x, y)$ is abr. Therefore, from the change of variable theorem we have that:

$$\text{Area}(E) = \iint_E \mathrm{d}x\,\mathrm{d}y = \int_0^{2\pi}\int_0^1 abr\,\mathrm{d}r\,\mathrm{d}t = \pi ab \tag{11}$$

□

3 Introduction to astrodynamics and satellite tracking

3.1 The two body problem

3.1.1 Trajectory equation

We are interested in understanding the dynamics of a spacecraft in orbit around the Earth. These dynamics are governed by Newton's second law of motion, which assuming that both the Earth and the spacecraft are point masses (see Section 4 for a more realistic model), this can be written as

$$\ddot{\mathbf{r}} = -\frac{GM_\oplus}{r^2}\mathbf{e}_r \tag{12}$$

where the mass of the satellite has been canceled out on both sides of the equation. Here, $\mathbf{r}$ is the position vector (also called *radius vector*) of the spacecraft with respect to the center of the Earth, $r := \|\mathbf{r}\|$, $\mathbf{e}_r = \frac{\mathbf{r}}{r}$ is the unit vector in the direction of $\mathbf{r}$, $M_\oplus \simeq 5.972 \times 10^{24}$ kg is the mass of the Earth, and $G \simeq 6.674 \times 10^{-11}$ $\mathrm{m}^3/(\mathrm{kg}\cdot\mathrm{s}^2)$ is the universal gravitational constant. Note that the minus sign is due to the fact that the gravitational force is attractive, i.e. pointing towards the Earth. Here and throughout the document the *dot notation* $\ddot{\mathbf{r}}$ means that the derivatives are taken with respect to time. Cross-multiplying Eq. (12) by $\mathbf{r}$, we obtain

$$\frac{\mathrm{d}(\mathbf{r}\times\dot{\mathbf{r}})}{\mathrm{d}t} = \dot{\mathbf{r}}\times\dot{\mathbf{r}} + \mathbf{r}\times\ddot{\mathbf{r}} = -\frac{GM_\oplus}{r^3}(\mathbf{r}\times\mathbf{r}) = 0 \tag{13}$$

Hence $\mathbf{h} := \mathbf{r}\times\dot{\mathbf{r}}$ is constant. The physical consequence is that the motion of the spacecraft around the Earth is confined to a plane, called the *orbital plane*, because the position $\mathbf{r}$ and velocity $\dot{\mathbf{r}}$ are always perpendicular to $\mathbf{h}$.

We are interested now in what kind of curves may be described by a spacecraft orbiting the Earth, when considered both objects as point masses. That is, we want to somehow isolate $\mathbf{r}$ (or r) from Eq. (12). It is standard in Astrodynamics to denote $\mu := GM_\oplus$.

Proposition 7 (Kepler's first law). Consider two point-mass bodies. The motion of one body orbiting the other can be described by a conic section. Hence, it can be expressed in the form:

$$r(t) = \frac{p}{1+e\cos(\nu(t))} = \frac{h^2/\mu}{1+(B/\mu)\cos(\nu(t))} \tag{14}$$

for some parameters $p = h^2/\mu$, $e = B/\mu$ and B.

Proof. Cross-multiplying Eq. (12) by $\mathbf{h}$ we obtain

$$\frac{\mathrm{d}(\dot{\mathbf{r}}\times\mathbf{h})}{\mathrm{d}t} = \ddot{\mathbf{r}}\times\mathbf{h} = -\frac{\mu}{r^3}\mathbf{r}\times\mathbf{h} = -\frac{\mu}{r^3}\mathbf{r}\times(\mathbf{r}\times\dot{\mathbf{r}}) = \frac{\mu}{r^3}[(\mathbf{r}\cdot\mathbf{r})\dot{\mathbf{r}} - (\mathbf{r}\cdot\dot{\mathbf{r}})\mathbf{r}] \tag{15}$$

where in the last equality we have used the vector equality $\mathbf{u}\times(\mathbf{v}\times\mathbf{w}) = (\mathbf{u}\cdot\mathbf{w})\mathbf{v} - (\mathbf{u}\cdot\mathbf{v})\mathbf{w}$ for $\mathbf{u},\mathbf{v},\mathbf{w}\in\mathbb{R}^3$. Now note that:

$$\frac{\mathrm{d}}{\mathrm{d}t}\left(\frac{\mathbf{r}}{r}\right) = \frac{\dot{\mathbf{r}}}{r} - \frac{\dot{r}}{r^2}\mathbf{r} = \frac{1}{r^3}[(\mathbf{r}\cdot\mathbf{r})\dot{\mathbf{r}} - (\mathbf{r}\cdot\dot{\mathbf{r}})\mathbf{r}] \tag{16}$$

because[3] $2r\dot{r} = \dfrac{\mathrm{d}(r^2)}{\mathrm{d}t} = \dfrac{\mathrm{d}(\mathbf{r}\cdot\mathbf{r})}{\mathrm{d}t} = 2\mathbf{r}\cdot\dot{\mathbf{r}}$. Thus:

$$\frac{\mathrm{d}(\dot{\mathbf{r}}\times\mathbf{h})}{\mathrm{d}t} = \mu\frac{\mathrm{d}}{\mathrm{d}t}\left(\frac{\mathbf{r}}{r}\right) \tag{17}$$

Integrating with respect to the time yields

$$\dot{\mathbf{r}}\times\mathbf{h} = \frac{\mu}{r}\mathbf{r} + \mathbf{B} \tag{18}$$

[3]Bear in mind that in general $\dot{r} \neq \|\dot{\mathbf{r}}\|$. Indeed, if β denotes the angle between $\mathbf{r}$ and $\dot{\mathbf{r}}$ we have that $\dot{r} = \|\dot{\mathbf{r}}\|\cos\beta$. In particular $\dot{r}$ may be negative.

where $\mathbf{B} \in \mathbb{R}^3$ is the constant of integration. Observe that since $\dot{\mathbf{r}} \times \mathbf{h}$ is perpendicular to $\mathbf{h}$, $\dot{\mathbf{r}} \times \mathbf{h}$ lies on the orbital plane and so does $\mathbf{r}$. Hence, $\mathbf{B}$ lies on the orbital plane too. Now, dot-multiplying this last equation by $\mathbf{r}$ and using that $\mathbf{u} \cdot (\mathbf{v} \times \mathbf{w}) = (\mathbf{u} \times \mathbf{v}) \cdot \mathbf{w}$ $\forall \mathbf{u}, \mathbf{v}, \mathbf{w} \in \mathbb{R}^3$ we obtain

$$h^2 = \mathbf{h} \cdot \mathbf{h} = (\mathbf{r} \times \dot{\mathbf{r}}) \cdot \mathbf{h} = \mathbf{r} \cdot (\dot{\mathbf{r}} \times \mathbf{h}) = \frac{\mu}{r}\mathbf{r} \cdot \mathbf{r} + \mathbf{r} \cdot \mathbf{B} = \mu r + rB\cos\nu \tag{19}$$

where $h := \|\mathbf{h}\|$, $B := \|\mathbf{B}\|$ and ν denotes the angle between $\mathbf{r}$ and $\mathbf{B}$, called *true anomaly*. Rearranging the terms we finally obtain the equation of a conic section

$$r = \frac{h^2/\mu}{1 + (B/\mu)\cos(\nu)} \tag{20}$$

with $p := h^2/\mu$ and $e := B/\mu$. □

From here on, let's assume that B is small enough to satisfy $e < 1$, as this is our primary case of interest. We've seen in Section 2.2 the range of values that can r take in that case, and we deduced an equation for the semi-major axis. Note that this latter quantity can also be expressed as:

$$a = \frac{r_{\max} + r_{\min}}{2} = \frac{p}{1 - e^2} = \frac{h^2}{\mu(1 - e^2)} \tag{21}$$

Observe that at $\mathbf{r}_{\min}$, we have $\nu = 0$ and so $\mathbf{r} \parallel \mathbf{B}$ at this point. Hence, $\mathbf{B}$ points towards the periapsis of the orbit.

Definition 8. Let $\mathbf{r}(t)$ be the position of the spacecraft at time t and $A(t)$ be the area swept by the radius vector $\mathbf{r}(t)$ in the time interval $[0, t]$. We define the *areal velocity* as $\frac{\mathrm{d}A(t)}{\mathrm{d}t}$.

Proposition 9 (Kepler's second law). The areal velocity remains constant, namely:

$$\frac{\mathrm{d}A(t)}{\mathrm{d}t} = \frac{h}{2} \tag{22}$$

Proof. Recall that the area of a parallelogram generated by two vectors $\mathbf{u}, \mathbf{v} \in \mathbb{R}^3$ is given by $\|\mathbf{u} \times \mathbf{v}\|$. Thus, approximating the difference $A(t+k) - A(t)$ by half of the area of the parallelogram generated by $\mathbf{r}(t)$ and $\mathbf{r}(t+k)$ (see Fig. 5) we obtain:

$$\frac{\mathrm{d}A(t)}{\mathrm{d}t} = \lim_{k\to 0} \frac{A(t+k) - A(t)}{k} = \lim_{k\to 0} \frac{\|\mathbf{r}(t) \times \mathbf{r}(t+k)\|}{2k} = \lim_{k\to 0} \frac{\|\mathbf{r}(t) \times (\mathbf{r}(t+k) - \mathbf{r}(t))\|}{2k} =$$
$$= \frac{\|\mathbf{r}(t) \times \dot{\mathbf{r}}(t)\|}{2} = \frac{h}{2} \tag{23}$$

where the penultimate equality is due to the continuity and linearity of the cross product. □

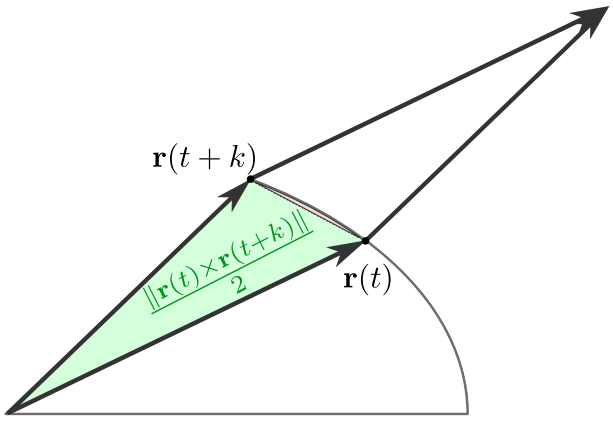

Figure 5: Graphical representation of the error made (red region) when approximating the area swept by the radius vector by half the area of the parallelogram generated by $\mathbf{r}(t)$ and $\mathbf{r}(t+k)$ (green region).

Definition 10. Let T be the orbital period of the satellite. We define the *mean motion* as $n := 2\pi/T$.

Proposition 11 (Kepler's third law). The mean motion is related to the semi-major axis by:

$$n = \sqrt{\frac{\mu}{a^3}} \tag{24}$$

Proof. Integrating Eq. (22) with respect to time between 0 and T (the period) yields:

$$\pi ab = A(T) = \int_0^T A'(t)\,\mathrm{d}t = \int_0^T \frac{h}{2}\,\mathrm{d}t = \frac{hT}{2} \implies n = \frac{2\pi}{T} = \frac{h}{ab} = \frac{h}{a^2\sqrt{1-e^2}} = \sqrt{\frac{\mu}{a^3}} \tag{25}$$

where we have used Eqs. (7) and (21). □

3.1.2 Kepler's equation

So far we have been able to describe the geometry of motion of a body orbiting another one. However, we have not been concerned about the specific position of the body as a function of time. That is, how to obtain $\nu(t)$ at each instant of time. In order to do this, we may think the area A as a function of ν, that measures the area swept by the radio vector from an initial instant ν_0. Thus, we know that:

$$A(\nu) = \int_{\nu_0}^{\nu}\int_0^{r(\theta)} r\,\mathrm{d}r\,\mathrm{d}\theta = \int_{\nu_0}^{\nu} \frac{r(\theta)^2}{2}\,\mathrm{d}\theta \implies \frac{\mathrm{d}A}{\mathrm{d}\nu} = \frac{r^2}{2} \tag{26}$$

Using the chain rule and Eq. (22) we obtain that:

$$\frac{h}{2} = \frac{\mathrm{d}A}{\mathrm{d}t} = \frac{\mathrm{d}A}{\mathrm{d}\nu}\frac{\mathrm{d}\nu}{\mathrm{d}t} = \frac{r^2}{2}\dot{\nu} \tag{27}$$

So from Eqs. (14) and (27), we get the following differential equation that must satisfy ν:

$$\dot{\nu} = \frac{h}{r^2} = \frac{h}{p^2}(1 + e\cos\nu)^2 \tag{28}$$

This equation, when integrated with respect to the time, lead us to an elliptic integral which can be very computationally expensive. Our goal in this section is to find an easier way to compute the exact position of the satellite at each instant of time [MG05]. This will lead us to the so-called *Kepler's equation*. For this purpose we are forced to introduce a new parameter, E, called *eccentric anomaly*. It is defined as the angle between the segment from the origin of the ellipse to the periapsis and the line passing through the center of the ellipse and the point in a circle (of radius a and same center as the ellipse) which is just above the position of the satellite (see Fig. 6). Clearly, using the reference frame of Fig. 6, the position

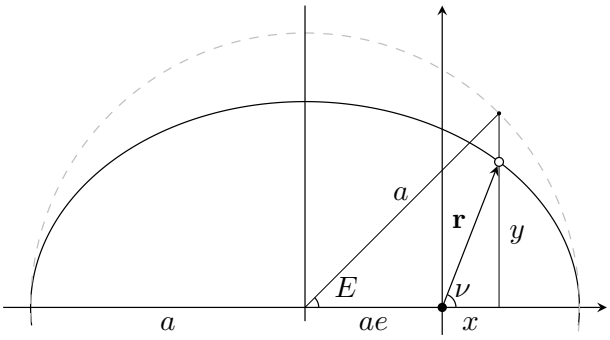

Figure 6: Ellipse orbit of the satellite together with an auxiliary circle of radius a needed to define the eccentric anomaly.

of the satellite is determined by $x = r\cos\nu$, $y = r\sin\nu$. But we would like to find an expression of x and y in terms of E rather than ν. To do this, note that $a\cos E = ae + x$, so:

$$x = a(\cos E - e) \tag{29}$$

We can also get an expression of r in terms of E by solving the equation:

$$r = \frac{p}{1 + e\cos\nu} = \frac{a(1-e^2)}{1 + e\frac{x}{r}} = \frac{ra(1-e^2)}{r + ae(\cos E - e)} \implies r = a(1 - e\cos E) \tag{30}$$

Finally from Eqs. (29) and (30) we get:

$$y^2 = r^2 - x^2 = a^2(1-e^2)(\sin E)^2 \implies y = a\sqrt{1-e^2}\sin E \tag{31}$$

Expressing now the areal velocity h as a function of E we have:

$$\begin{aligned} h &= x\dot{y} - y\dot{x} && (32)\\ &= a^2(\cos E - e)\sqrt{1-e^2}(\cos E)\dot{E} + a^2(\sin E)^2\dot{E}\sqrt{1-e^2} && (33)\\ &= a^2\sqrt{1-e^2}\dot{E}(1 - e\cos E) && (34) \end{aligned}$$

From Eq. (21) we know that $h = \sqrt{\mu a(1-e^2)}$. Thus, substituting this into Eq. (34) we deduce that E must satisfy the following differential equation:

$$\dot{E}(1 - e\cos E) = \sqrt{\frac{\mu}{a^3}} = n \tag{35}$$

where the last equality follows from Proposition 11. Integrating this equation with respect to the time yields the *Kepler's equation*:

$$E(t) - e\sin E(t) = n(t - t_0) \tag{36}$$

where t_0 is the time at which E vanishes. Using the reference frame of Fig. 6 (also known as the perifocal frame, see Definition 24) this corresponds to the time at which the satellite is at the perigee. The value $M := n(t - t_0)$ is called *mean anomaly*. Note that, contrarily to E and ν, the mean anomaly increases linearly with time.

Kepler's equation is the key to solve the problem of finding the position of the satellite at each instant of time. Later on we will discuss techniques to effectively solve this equation for E, given e and M.

3.2 Time and reference systems

3.2.1 Julian day

The measurement of time has undergone significant changes throughout the centuries, and its interpretation continues to vary across different cultures. Astronomy, however, has always needed a universal time measurement system and easy-to-work with. In view of this, the so-called *Julian date* is used as the standard day-counting system in astronomy.

Definition 12 (Julian date). The *Julian date* (JD) is the number of days, of length $24 \cdot 3\,600 = 86\,400$ seconds, elapsed since the beginning of the *Julian period*, that is, since January 1, 4713 BC, at 12:00 (noon) in the Julian calendar[4]. A *Julian year* is defined as 365.25 days and therefore a *Julian century* as 36 525 days.

As the unit of second is not constant among the time systems that we will use throughout the document (UT1, TT, UTC, etc.) (see Section 3.2.2), the actual length of a JD will vary depending on the time system used. We will distinguish them by adding a subscript to the JD, for instance $\mathrm{JD}_{\mathrm{UT1}}$, $\mathrm{JD}_{\mathrm{TT}}$ or $\mathrm{JD}_{\mathrm{UTC}}$. Later on, we will give formulas that relate these time systems, and usually they will be expressed as the number of Julian centuries elapsed since January 1, 2000, at 12:00 TT (noon) in the Julian calendar. This number is given by:

$$\frac{\mathrm{JD} - 2\,451\,545}{36\,525} \tag{37}$$

Here 2 451 545 corresponds to the Julian date of January 1, 2000, at 12:00 TT (noon).

[4] According to [Val13], the convention to start the JD at noon each day benefits astronomers (who often work at night) because they can make all their observations on a single day.

3.2.2 Time measurement

As human beings we are naturally interested in how time passes and therefore the correct measure of it becomes an essential necessity for us. As it is the Sun that governs our daily activity, it is natural to define time from it. But first we need some preliminary definitions:

Definition 13. We define the *equatorial plane* as the plane in $\mathbb{R}^3$ that contains the Earth equator. We define the *ecliptic plane* as the orbital plane in $\mathbb{R}^3$ of the Earth around the Sun.

Definition 14. We define the *celestial sphere* as an abstract sphere of infinite radius centered at the center of mass of the Earth. All the celestial objects are thus projected naturally on the celestial sphere, identifying them with two spherical coordinates, known as *right ascension* and *declination*, which we define below. The intersection of the equatorial plane with the celestial sphere is called *celestial equator*. The intersection of the ecliptic plane with the celestial sphere is called *ecliptic* (see Fig. 7 for a better understanding).

A first important thing to note is that, since the celestial sphere is centered at the Earth, the Sun moves along the ecliptic. Moreover, note that both the celestial equator and the ecliptic are two different great circles on the celestial sphere. Hence, they intersect at exactly two points.

Definition 15. Consider the two points of intersection between the celestial equator and the ecliptic. We define the *vernal equinox* as the point Υ, from these two, where the Sun crosses the celestial equator from south to north.

The angle measured along the equator of any object on the celestial sphere from the vernal equinox is called *right ascension*, whereas the angle measured along the meridian of the object from the position of the object to the equator is called *declination* (see Fig. 7).

An *apparent solar day* is defined to be the time between two successive transits of the Sun across our local meridian[5]. One should note that the Earth has to rotate on itself slightly more than one revolution in order to complete one apparent solar day (see Fig. 8). In addition, due to the non-circular orbit of the Earth around the Sun, the length of an apparent solar day is not constant, as the Earth has to rotate on itself slightly more in the perihelion than in the aphelion, where it goes faster. The *apparent sidereal day* is defined as the time it takes for the Earth to complete a rotation on itself (see Fig. 8 for a better understanding). From the point of view of the celestial sphere, the apparent solar time is the angle (measured along the celestial equator) between the local meridian and the meridian of the Sun at that epoch, which is not uniform because the angular velocity of the Earth (both in its orbit around the Sun and in its rotation around its own axis) is not constant [MG05].

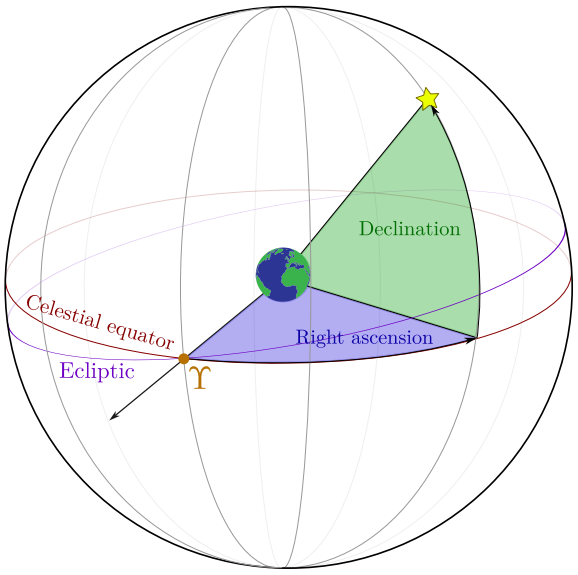

Figure 7: Right ascension and declination of a star in the celestial sphere

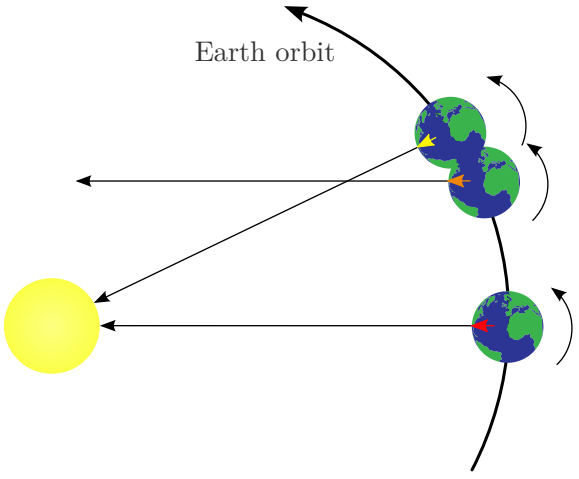

Figure 8: Graphical representation of the difference between a solar day (yellow) and a sidereal day (orange). (not to scale)

[5] We consider the local meridian as the meridian on the celestial sphere that is projected onto the Earth and moves in synchronization with it.

Due to Kepler's second law, the Earth's non-circular orbit around the Sun results in some days being shorter than others. As a result, the actual position of the Sun is not ideal for precise time measurement. The introduction of a *mean Sun* is, thus, a necessity.

Definition 16. The *mean Sun* is a fictitious Sun that moves along the celestial equator at a constant rate [Val13]. This rate is determined in order to make the real Sun and the mean Sun coincide at the vernal equinox. We define the *mean solar time* as the hour angle (along the celestial equator) between the local meridian and the meridian of the mean Sun.

It is worth noting that unlike the real Sun, the mean Sun moves along the celestial equator, rather than the ecliptic.

Definition 17. We define the *prime meridian* or *zero meridian* as the meridian on the celestial sphere that passes through the Royal Observatory in Greenwich, England (when projected onto the Earth).

Definition 18. The *Greenwich Mean Time* (GMT) or *Universal Time* (UT) is the hour angle of the mean Sun measured from the prime meridian and counted from midnight. That is, when the prime meridian and mean Sun meridian coincide (noon), the GMT is 12:00.

The use of two distinct names, namely GMT and UT, to refer to the same time can be attributed to historical reasons. Initially, GMT was defined as the mean solar time at the prime meridian with 00:00 GMT coinciding with the moment when the mean Sun was at that meridian. On the other hand, UT was introduced as a 12-hour translation of GMT, intended for civilian purposes. Eventually, GMT was redefined to align with UT.

In the middle of the 20th century, *Ephemeris Time* (ET) was introduced to cope with the irregularities of the Earth's rotation (see Section 3.2.3). This time was defined from historical observations of planets in a Newtonian physics framework, isolating the time from the equations, and the origin of time was chosen coherently with GMT, at January 0, 1900, 12:00 GMT (JD 2 415 020.0). This timescale provided a uniform time, although it was more difficult to measure than the mean solar time. In the meantime, atomic clocks were invented and at 1967 *atomic time* (TAI, from French *Temps Athomique International*) was adopted as the SI unit of second. The origin was chosen such that TAI matched UT at the 00:00 UT of January 1, 1958, and at that time ET was displaced from UT by 32.184 seconds. At the end of the 20th century, *Terrestrial Time* (TT) was introduced within a relativistic framework in order to replace ET and provide a smooth and more accurate continuation of it yielding the relation [MG05]:

$$\mathrm{TT} = \mathrm{ET} = \mathrm{TAI} + 32.184\,\mathrm{s} \tag{38}$$

For astronomical calculations, it is convenient to consider a timescale defined directly from Earth's rotation, known as *sidereal time*. Namely, *Greenwich Mean Sidereal Time* (GMST) is defined as the angle between the prime meridian and the mean vernal equinox of date (see Section 3.2.3). Due to unpredictable irregular changes on the rotation of the Earth, GMST cannot be computed directly with a formula in terms of TAI or TT.

Universal Time 1 (UT1) is the presently used form of Universal time, and it is defined in terms of Earth's rotation with the following deterministic formula given in [Aok+81]. For each day, 00:00 UT1 is defined as the time instant in which GMST has the value:

$$\mathrm{GMST}(0\mathrm{h\ UT1}) = 24\,110.548\,41 + 8\,640\,184.812\,866 T_{\mathrm{UT1},0} + 0.093\,104 {T_{\mathrm{UT1},0}}^2 - 6.2 \cdot 10^{-6} {T_{\mathrm{UT1},0}}^3 \tag{39}$$

where $T_{\mathrm{UT1},0} = \frac{\mathrm{JD(0h\ UT1)} - 2\,451\,545}{36\,525}$ denotes the number of Julian centuries that have passed since January 2000, 1.5 UT1 at the beginning of the day. The units of the coefficients are seconds. For any instant of time during the day, the following formula is used:

$$\begin{aligned}\mathrm{GMST(UT1)} = 24\,110.548\,41 + 8\,640\,184.812\,866 T_{\mathrm{UT1}} + 1.002\,737\,909\,350 \cdot 240\mathrm{UT1} + \\ + 0.093\,104 {T_{\mathrm{UT1}}}^2 - 6.2 \cdot 10^{-6} {T_{\mathrm{UT1}}}^3\end{aligned} \tag{40}$$

where $T_{\mathrm{UT1}} = \frac{\mathrm{JD(UT1)} - 2\,451\,545}{36\,525}$ and UT1 are measured in seconds. The coefficient $\omega := 1.002\,737\,909\,350$ is the Earth's mean angular velocity in degrees per second and the coefficient $240 = \frac{3\,600}{15}$ is the number of seconds in one degree[6]. Similarly to GMST, there is no simple conversion between UT1 and TT or

[6] Recall that $15^\circ = 1\,\mathrm{h}$, $60' = 1^\circ$, $60'' = 1'$, where $''$ are arc seconds and $'$ are arc minutes.

TAI. Instead, IERS[7] (*International Earth Rotation and Reference Systems Service*) provides regularly a bulletin with the difference $\Delta T := \text{TT} - \text{UT1}$ at several dates. Interpolating these values we can obtain UT1 from TT at any epoch.

Finally, our everyday clock is based on *Coordinated Universal Time* (UTC, from French *Temps Universel Coordonné*). It is defined to be as uniform as TAI but always kept closer than 0.9 seconds to UT1 in order to resemble a mean solar time (see Fig. 9). Scientists achieve this by introducing a *leap second* (see Fig. 10), which is an extra second added to UTC at irregular intervals. Fig. 9 summarizes some time systems introduced in the document.

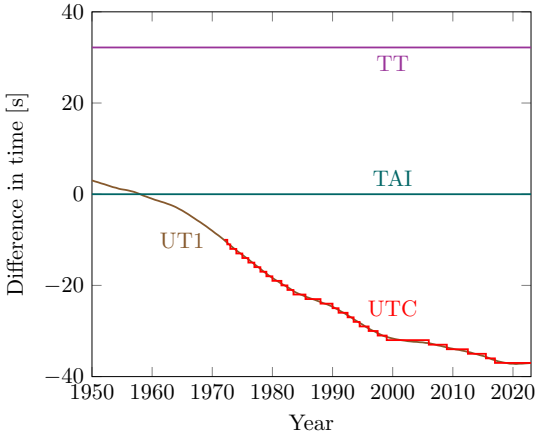

Figure 9: Evolution of times TT, UT1 and UTC in comparison with TAI. [Obsa]

```
1998 December 31,       23h 59m 59s
1998 December 31,       23h 59m 60s
1999 January   1,       00h 00m 00s
1999 January   1,       00h 00m 01s
```

Figure 10: Leap second introduced to UTC time at the end of the December 1998. [RS98b]

We summarize here useful conversions between time systems:

$$\text{GMST(UT1)} = 24\,110.548\,41 + 8\,640\,184.812\,866 T_{\text{UT1}} + 1.002\,737\,909\,350 \cdot 240\text{UT1} + \\ + 0.093\,104 {T_{\text{UT1}}}^2 - 6.2 \cdot 10^{-6} {T_{\text{UT1}}}^3$$

$$\begin{aligned} \text{UT1} &= \text{TT} - \Delta T \\ \text{TT} &= \text{TAI} - 32.184 \\ \text{TAI} &= \text{UTC} + \delta \end{aligned}$$

where ΔT is the difference between TT and UT1, and δ is a piecewise constant function that counts the number of leap seconds introduced since 1972, when they were introduced for the first time. All the numbers have units of second.

3.2.3 Reference systems

It is well-known that Newton's second law is only valid when applied to an *inertial reference frame*, that is, a frame of reference that is not undergoing any acceleration. In practice, however, almost any frame of reference is non-inertial. In this chapter we will describe a quasi-inertial frame of reference which will be used to integrate Newton's second law. On the other hand, since the Earth is not a body with a homogeneous density of mass, there are zones with higher mass density than others, and therefore with higher gravitational pull (see Section 4.2.3). Therefore, we will need the longitude and latitude of the satellite with respect to a fixed Earth at each time of integration.

Based on our study of satellite motion around the Earth, it is natural to place all the origins of the reference frames considered throughout the document at the center of mass of the Earth.

The first reference frame we must consider is the *celestial* one. In the celestial frame, the x-axis is defined as the line of intersection between the equatorial plane and the ecliptic plane. The positive direction is chosen to point towards the vernal equinox. The z-axis is chosen to be perpendicular to the equatorial plane and the y-axis is such that the triplet (x, y, z) is a right-handed system.

However, due to the presence of other solar system planets (and other smaller perturbations), the orbital plane of the Earth is not fixed in space, but is subjected to a small variation called *planetary precession*.

[7] More information on https://www.iers.org (accessed on June 8, 2023).

Moreover, the gravitational attraction of the Sun and Moon on the Earth's equator cause Earth's axis of rotation to precess similarly to the action of a spinning top with a period of about 26 000 years [MG05]. This motion is called *lunisolar precession*. On the other hand, smaller perturbations in amplitude and shorter period (around 18.6 years [Wika]) superposed with the precessional motion creates a motion called *nutation*. When this latter oscillations are averaged out, the vernal equinox and the equator are referred to *mean* values, rather than *true* values.

In addition, the Earth's axis of rotation undergoes a slight periodic motion around a reference axis of rotation, that passes through the *IRP* (*IERS Reference Pole*). This motion is called *polar motion* and is caused by the redistribution of the Earth's mass due to the seasonal variations of the atmosphere and the oceans. The polar motion is usually described by the *CIP* (*Celestial Intermediate Pole*), which is the intersection of the Earth's axis of rotation with the celestial sphere. In Fig. 11 we summarize the different types of perturbations on the Earth's axis of rotation.

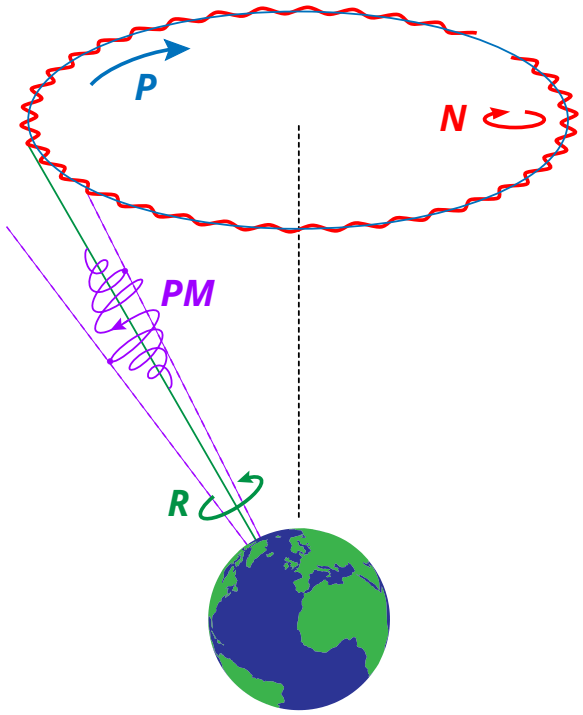

Figure 11: Graphical explanation of the perturbation by precession (blue), nutation (red) and polar motion (violet) of the Earth's axis of rotation (green).

In view of this time-dependent orientation of both the ecliptic and the equator, the standard-reference frame chosen is based on the mean equator, ecliptic and mean equinox of a fixed time, the beginning of the year 2000, namely at 12:00 TT on January 1, 2000, the so-called *J2000 epoch*.

Definition 19 (Earth-centered inertial frame). We define the *J2000 reference frame* as the reference frame whose x-axis is the intersection of the mean celestial equator and the ecliptic of the J2000 epoch, pointing at the mean vernal equinox of the same epoch; the z-axis is perpendicular to the mean equator of that epoch, and the y-axis is chosen such that the triplet (x, y, z) is a right-handed system. This frame of reference is also called *Earth-centered inertial* (ECI) frame.

Let's introduce now an Earth-fixed reference frame.

Definition 20 (Earth-centered, Earth-fixed frame). We define the *Earth-centered, Earth-fixed frame of reference* (ECEF) as the frame of reference whose z-axis is pointing towards the IRP; the x-axis is contained in the plane perpendicular to the z-axis and pointing to the prime meridian, and the y-axis is chosen such that the triplet (x, y, z) is a right-handed system.

These two coordinate systems have, as mentioned earlier, the origin at the center of mass of the Earth. Note that the ECEF frame is non-inertial, since it is rotating with the Earth. Similarly, the ECI frame is also non-inertial due to the annual motion of the Earth around the Sun. Thus, it is subjected to a certain acceleration, but it can be thought as inertial over short periods of time.

3.2.4 Conversion between reference systems

As we noted in the previous section the angle ε between the celestial equator and ecliptic planes is not constant due to the planetary precession.

Our goal in this section is to transform the position of the satellite from the ECI system to the ECEF system and vice versa. This rotation transformation is given by a product of 4 rotations matrices:

- the precession matrix $\mathbf{P}$,
- the nutation matrix $\mathbf{N}$,
- the Earth rotation matrix $\mathbf{\Theta}$, and
- the polar motion matrix $\mathbf{\Pi}$.

These matrices are such that:

$$\mathbf{r}_{\text{ECEF}}(t) = \mathbf{\Pi}(t)\mathbf{\Theta}(t)\mathbf{N}(t)\mathbf{P}(t)\mathbf{r}_{\text{ECI}}(t) \tag{41}$$

where $\mathbf{r}_{\text{ECEF}}(t)$ is the position vector of the satellite in the ECEF frame at time t and $\mathbf{r}_{\text{ECI}}(t)$ is the position vector of the satellite in the ECI frame at time t. From here on, we will omit the evaluation on the time t for the sake of simplicity. Let's now argue why the transformation has this particular form.

The precession matrix is responsible for *eliminating* all the movement due to the planetary and lunisolar precession. Thus, $\mathbf{P}$ transforms the mean equator and mean equinox at time J2000 to the respective values at time t. With the help of Fig. 12, one can check that this transformation is given by:

$$\mathbf{P} = \mathbf{R}_z(-90 - z)\mathbf{R}_x(\theta)\mathbf{R}_z(90 - \zeta) \tag{42}$$

And with a bit of algebra it can be simplified to:

$$\mathbf{P} = \mathbf{R}_z(-z)\mathbf{R}_y(\theta)\mathbf{R}_z(-\zeta) \tag{43}$$

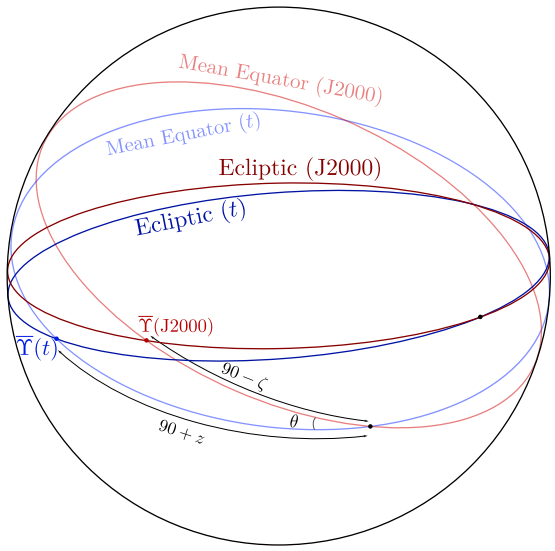

Figure 12: Celestial sphere showing the ecliptic and the equator of both the epoch J2000 and the current epoch t. Dark colors represent the ecliptic while light colors represent the equator. On the other hand, red colors represents the J2000 epoch and blue colors represents the current epoch t. Based on [MG05].

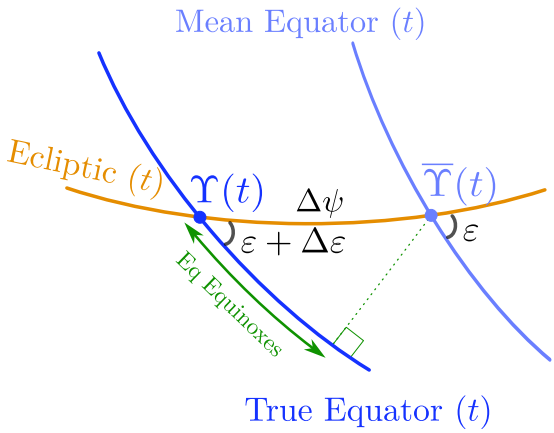

Figure 13: True and mean equators, and true and mean equinoxes (Υ and $\overline{\Upsilon}$, respectively) at a given epoch t together with the ecliptic at that time. Based on [MG05].

Recall that the fundamental rotation matrices $\mathbf{R}_x(\theta)$, $\mathbf{R}_y(\theta)$ and $\mathbf{R}_z(\theta)$ are with respect to the axis of the J2000 frame, and they are given by:

$$\mathbf{R}_x(\varphi) = \begin{pmatrix} 1 & 0 & 0 \\ 0 & \cos\varphi & \sin\varphi \\ 0 & -\sin\varphi & \cos\varphi \end{pmatrix} \quad \mathbf{R}_y(\varphi) = \begin{pmatrix} \cos\varphi & 0 & -\sin\varphi \\ 0 & 1 & 0 \\ \sin\varphi & 0 & \cos\varphi \end{pmatrix} \quad \mathbf{R}_z(\varphi) = \begin{pmatrix} \cos\varphi & \sin\varphi & 0 \\ -\sin\varphi & \cos\varphi & 0 \\ 0 & 0 & 1 \end{pmatrix} \tag{44}$$

where we have used the convention of signs given by [GPS02]. The reader may wonder why we have used the notation $90 - z$ and $90 - \zeta$ instead of z and ζ (for example) for the angles in question. The reason is related to the precise definition of these angles from the pole of the celestial sphere rather than from where we have defined them, but we will not elaborate on this point here. Nonetheless, we have chosen this notation to maintain consistency with related articles [Lie+77].

The nutation perturbations are ruled out by the nutation matrix $\mathbf{N}$. This matrix transforms the coordinates of the mean equator and equinox at epoch t to those of the true equator and equinox at the same epoch, respectively. Hence, from figure Fig. 13 we can see that the nutation matrix is given by:

$$\mathbf{N} = \mathbf{R}_x(-\varepsilon - \Delta\varepsilon)\mathbf{R}_z(-\Delta\psi)\mathbf{R}_x(\varepsilon) \tag{45}$$

In Section 3.2.2 we defined the GMST as the hour angle between the mean vernal equinox and the prime meridian, measured on the true equator. Similarly, we define the *Greenwich Apparent Sidereal Time* (GAST) as the hour angle between the true vernal equinox and the prime meridian, measured on the true equator too. The difference between these two times is given by the so-called *equation of the equinoxes*, which up to first order in the nutation angles is given by (see Fig. 13):

$$\text{GAST} - \text{GMST} \simeq \Delta\psi \cos(\varepsilon + \Delta\varepsilon) \tag{46}$$

The Earth rotation matrix $\mathbf{\Theta}$ is responsible for aligning satellites with their actual meridian at the time of the observation. This matrix is given by:

$$\mathbf{\Theta} = \mathbf{R}_z(\text{GAST}) \tag{47}$$

Finally the polar motion movement around the IRP axis is modelled with the matrix $\mathbf{\Pi}$ given by:

$$\mathbf{\Pi} = \mathbf{R}_y(-x_p)\mathbf{R}_x(-y_p) \tag{48}$$

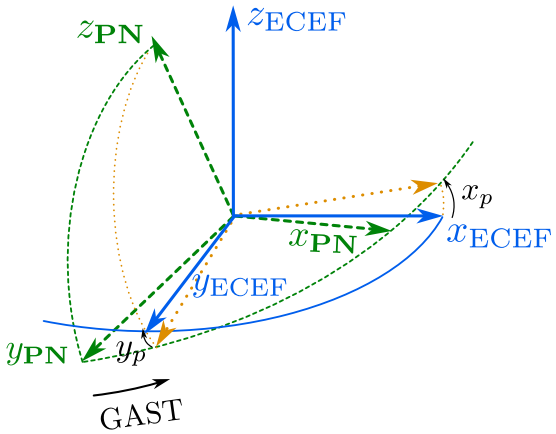

Figure 14: Three reference frames used to transform from the ECI frame to the ECEF frame. In green, the ECI frame once applied the precession and nutation transformations. In orange, the transformation of the green system once applied the rotation matrix $\mathbf{\Theta}$. Finally, in blue, the transformation of the orange system once applied the polar motion matrix $\mathbf{\Pi}$, that is, the ECEF frame.

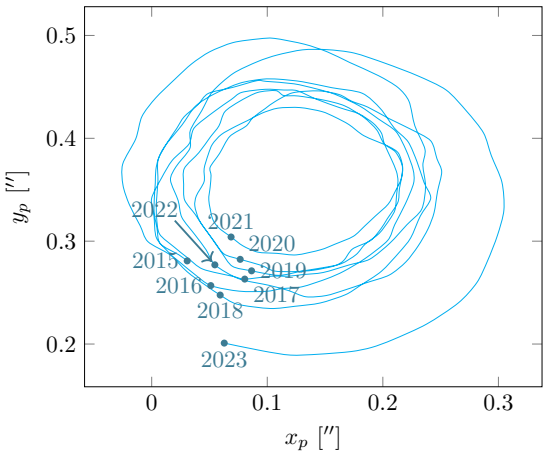

Figure 15: Graphical representation of evolution of the CIP with respect to IRP (placed at the origin of the graphic) due to polar motion. The blue dots indicate the position of the CIP at the beginning of the respective years. Data from [Obsb].

In Fig. 14 we can see a graphical representation of these two latter transformation matrices. The parameters x_p and y_p are constantly updated in the IERS bulletins [RS98a]. All the other parameters are given in [Lie+77], and we provide here a summary of them:

$$\varepsilon = 23.439\,291\,1^\circ - 46.815\,0''T - 0.000\,59''T^2 + 0.001\,813''T^3 \tag{49}$$

$$\zeta = 2\,306.218\,1'' + 0.301\,88''T + 0.017\,998''T^2 \tag{50}$$

$$\theta = 2\,004.310\,9''T - 0.426\,65''T^2 - 0.041\,833''T^3 \tag{51}$$

$$z = 2\,306.218\,1'' + 1.094\,68''T^2 + 0.018\,203''T^2 \tag{52}$$

where $T = \frac{\mathrm{JD}_{TT} - 2\,451\,545}{36\,525}$ are the Julian centuries that have elapsed since the J2000 epoch. The values for the nutations parameters $\Delta\psi$ and $\Delta\varepsilon$ can be expanded into [MG05]:

$$\Delta\psi = \sum_{i=1}^{106} (\Delta\psi)_i \sin\phi_i \qquad \Delta\varepsilon = \sum_{i=1}^{106} (\Delta\varepsilon)_i \cos\phi_i \tag{53}$$

where $\phi_i = p_{\ell,i}\ell + p_{\ell',i}\ell' + p_{F,i}F + p_{D,i}D + p_{\Omega,i}\Omega$; $p_{\ell,i}$, $p_{\ell',i}$, $p_{F,i}$, $p_{D,i}$, $p_{\Omega,i}$ are integer coefficients and the other variables are the Moon's mean anomaly (ℓ), the Sun's mean anomaly (ℓ'), the mean distance of the Moon from the ascending node (F), the difference between the mean longitudes of the Sun and the Moon (D), and the mean longitude of the ascending node of the Moon (Ω). We will not go into detail about these variables, there are explicit expressions for them in [MG05] as a function of $T = \frac{\mathrm{JD}_{TT} - 2\,451\,545}{36\,525}$:

$$\ell = 134°57'46.733'' + 477\,198°52'02.633''T + 31.310''T^2 + 0.064''T^3 \tag{54}$$

$$\ell' = 357°31'39.804'' + 35\,999°03'01.224''T - 0.577''T^2 - 0.012''T^3 \tag{55}$$

$$F = 93°16'18.877'' + 483\,202°01'03.137''T - 13.257''T^2 - 0.011''T^3 \tag{56}$$

$$D = 297°51'01.307'' + 445\,267°06'41.328''T - 6.891''T^2 + 0.019''T^3 \tag{57}$$

$$\Omega = 125°02'40.280'' - 1\,934°08'10.539''T + 7.455''T^2 + 0.008''T^3 \tag{58}$$

Some of these integer coefficients together with the values of the amplitudes $(\Delta\psi)_i$ and $(\Delta\varepsilon)_i$ are given in Table 1.

i	$p_{\ell,i}$	$p_{\ell',i}$	$p_{F,i}$	$p_{D,i}$	$p_{\Omega,i}$	$(\Delta\psi)_i$ $[0.0001'']$	$(\Delta\varepsilon)_i$ $[0.0001'']$
1	0	0	0	0	1	$-171\,996 - 174.2T$	$92\,025 + 8.9T$
2	0	0	0	0	2	$2\,062 + 0.2T$	$-895 + 0.5T$
3	−2	0	2	0	1	46	−24
4	2	0	−2	0	0	11	0
5	−2	0	2	0	2	−3	1
6	1	−1	0	−1	0	−3	0
7	0	−2	2	−2	1	−2	1
8	2	0	−2	0	1	1	0
9	0	0	2	−2	2	$-13\,187 - 1.6T$	$5\,736 - 3.1T$
⋮	⋮	⋮	⋮	⋮	⋮	⋮	⋮

Table 1: First nutation coefficients [MG05]

3.3 Keplerian orbital elements

In this section we will introduce the Keplerian orbital elements, which are a set of variables that completely determine the orbit of a satellite and, therefore, they are very useful in the storage of the orbital information of a satellite.

3.3.1 Keplerian orbital elements from position and velocity

We first give some preliminary definitions.

Definition 21. Consider a satellite orbiting the Earth. The *orbital plane* is the plane that contains the orbit of the satellite. The *line of nodes* is the line of intersection between the orbital plane and the equatorial plane. Finally, the *ascending node* ☊ is the point on the line of nodes and the orbit of the satellite where the satellite crosses the equatorial plane from south to north.

Definition 22 (Orbital elements). The *Keplerian orbital elements* of a satellite are five independent quantities that completely determine its orbit. If moreover the exact position of the satellite on the orbit is wanted, a sixth quantity is needed. The first five orbital elements are:

1. The *semi-major axis* a of the orbit.
2. The *eccentricity* e of the orbit.
3. The *inclination* i, which is the angle between the equatorial plane and the orbital plane.

4. The *longitude of the ascending node* Ω, which is the angle between the vernal equinox and the ascending node.
5. The *argument of perigee* ω, which is the angle between the ascending node and the periapsis, measured along the orbit.

The sixth quantity is the *true anomaly* ν, which is the angle between the periapsis and the position of the satellite on the orbit.

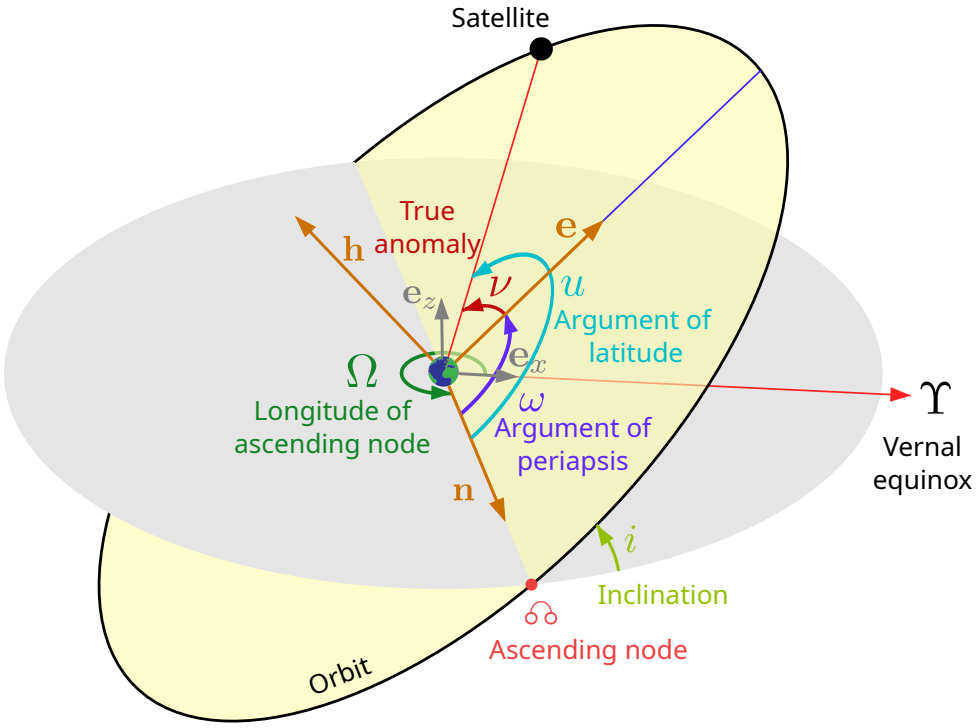

Figure 16: Orbital elements of a satellite. Based on [Las07].

Fig. 16 shows a schematic representation of these elements. The elements a, e and i are always well-defined. However, the elements Ω, ω and ν are not always well-defined, namely for $e = 0$ or $i = 0$. We discuss this in more detail below. For the moment assume $e \neq 0$ and $i \neq 0$. In order to express these elements in terms of the position and velocity of the satellite, we need to introduce the following vectors.

Definition 23. Let $\mathbf{e}_z = (0, 0, 1)$ be the unit vector perpendicular to the equatorial plane. We define the vector $\mathbf{n} := \mathbf{e}_z \times \mathbf{h}$ and the *eccentricity vector* $\mathbf{e}$ as $\mathbf{e} := \mathbf{B}/\mu$, whose norm is the eccentricity e.

Note that $\mathbf{n} \perp \mathbf{e}_z$ and $\mathbf{n} \perp \mathbf{h}$ which imply that $\mathbf{n}$ must lie on the orbital plane and equatorial plane, and therefore, in the line of nodes pointing towards the ascending node, by the right-hand rule. On the other hand, since $\mathbf{B}$ points towards the periapsis, so does $\mathbf{e}$. From here, let's obtain the orbital elements in terms of $\mathbf{r}$ and $\dot{\mathbf{r}}$.

First, we calculate $\mathbf{h} = \mathbf{r} \times \dot{\mathbf{r}}$. Now, note that the vectors $\mathbf{n}$ and $\mathbf{B}$ can be computed directly from $\mathbf{r}$, $\dot{\mathbf{r}}$ and $\mathbf{h}$. Thus, we can get e by taking the norm of $\mathbf{e}$. Then, looking at Fig. 16 one can check that the angles i, Ω, ω and ν are given by:

$$i = \arccos\left(\frac{\mathbf{h}\cdot\mathbf{e}_z}{h}\right) \quad \Omega = \arccos\left(\frac{\mathbf{n}\cdot\mathbf{e}_x}{n}\right) \quad \omega = \arccos\left(\frac{\mathbf{n}\cdot\mathbf{e}}{ne}\right) \quad \nu = \arccos\left(\frac{\mathbf{e}\cdot\mathbf{r}}{er}\right) \tag{59}$$

Here $\mathbf{e}_x = (1, 0, 0)$ denotes the basis unit vector that points towards the vernal equinox. By convention the angles i, Ω, ω are always given in the interval $[0, 2\pi)$, so in these formulas a small correction is needed when the angles are negative. The angle $\nu \in \mathbb{R}$ does not need any correction, because we will use it as a counter of the number of revolutions of the satellite. Finally, we can obtain a from Eq. (21):

$$a = \frac{h^2}{\mu(1 - e^2)} \tag{60}$$

Now we study the singular cases. If $e = 0$ (and therefore $\mathbf{e} = 0$) and $i \neq 0$, the orbit is called *circular inclined* [Val13]. In this case the elements ω, ν are not well-defined because there is no periapsis, or in other words, all the points lie at the same distance from the center of the Earth. To correct this we replace these variables by the *argument of latitude* u, which measures the angle between the ascending node and the position of the satellite on the orbit. The argument of latitude can be computed with the formula:

$$u = \arccos\left(\frac{\mathbf{n} \cdot \mathbf{r}}{nr}\right) \tag{61}$$

Note that in the case $e \neq 0$ and $i \neq 0$, $u = \omega + \nu$ (see Fig. 16). If $i = 0$ and $e \neq 0$, the orbit lies in the equatorial plane and it is called *elliptical equatorial*. Note that in this situation we have $\mathbf{n} = 0$ and the angles Ω and ω are undefined. By convention, we set $\Omega = 0$ and:

$$\omega = \arccos\left(\frac{\mathbf{e} \cdot \mathbf{e}_x}{e}\right) \tag{62}$$

If $e = 0$ and $i = 0$, the orbit is called *circular equatorial* and all these three variables (Ω, ω and ν) are undefined. In this case Ω is set to 0 and the other two variables are replaced with the *true longitude* λ, which is the angle between the vernal equinox and the position of the satellite on the orbit:

$$\lambda = \arccos\left(\frac{\mathbf{r} \cdot \mathbf{e}_x}{r}\right) \tag{63}$$

3.3.2 TLE sets

The positions of satellites are recorded and stored in a particular way, called *Two Line Element* sets (*TLEs*). TLEs consists of a two-line text with different data that facilitate the computation of position and velocity of the satellite at that specific instant of time. The following table summarizes all the information on it:

Line	Satellite number	Class	International designator			Epoch (UTC)		$\dot{n}/2$ [rev/day^2]	$\ddot{n}/6$ [rev/day^3]	B^* (drag term)	Model	TLE number	Checksum
			Year	Launch	Piece	Year	Day of the year (as fraction)						
1	55124	U	98	067	UR	23	086.16778994	S .01540407	S 14102-2	S 26634-2	0	999	1

Line	Satellite number	Inclination i [deg]	Right ascension Ω [deg]	Eccentricity e	Argument periapsis ω [deg]	Mean anomaly M [deg]	Mean motion n [rev/day]	Number of revolutions	Checksum
2	55124	51.6237	50.0017	0.0107578	188.3869	171.6963	16.01787819	13799	2

Table 2: TLE data set from the NUTSAT satellite. The white (empty) cells designate space characters and the green and yellow ones are used to distinguish consecutive data blocks. The cells labeled with S or E respresent cells reserved for the negative sign and the exponent of a number respectively, while the red dots in the middle of two cells denote that an implicit decimal point is assumed.

Let's clarify the meaning of some data blocks. The satellite number is a unique identifier assigned by NORAD (*North American Aerospace Defense Command*) for each earth-orbiting artificial satellite [Kel]. The classification of the satellite (Class) is divided into three categories: unclassified (U), classified (C), and secret (S). The international designator is comprised of three parts: the launch year (Year), the launch number of the year (Launch) and the piece of the launch (Piece). In the epoch block (Epoch), which indicates the time the Two-Line Elements (TLE) was generated, the first two digits represent the last two digits of the year, while the remaining portion represents the fractional day of the year, starting from 1. The model category refers to the orbital model used to generate the data, as specified in [Kel; Wikc]. The element set number (TLE number) is incremented by one when a new TLE is generated for this satellite. On the second line, the number of revolutions indicates the number of times the satellite has orbited the Earth since its launch. Finally, the checksum (modulo 10) is used to verify the integrity of the data[8].

3.3.3 Position and velocity in terms of the TLEs' orbital elements

We are now interested in proceed the other way around, that is, given the orbital elements from the TLE data, we want to compute the position and velocity of the satellite. In order to do that, we need to introduce the basis $(\mathbf{P}, \mathbf{Q}, \mathbf{W})$ linked to the orbit.

[8] Taking into account that the negative sign is counted as 1, and all the other cells without a number as 0.

Definition 24 (Perifocal coordinate system). Consider the orbit of a satellite. We define its associated *perifocal coordinate system* $(\mathbf{P}, \mathbf{Q}, \mathbf{W})$ as follows. The origin is on the Earth's center of mass. The unit vectors $\mathbf{P}$ and $\mathbf{Q}$ lie on the orbital plane and are such that $\mathbf{P}$ points towards the periapsis, that is $\mathbf{P} := \mathbf{B}/B$. The unit vector $\mathbf{W}$ is defined as $\mathbf{W} := \mathbf{h}/h$, that is perpendicular to the orbital plane, and $\mathbf{Q} := \mathbf{W} \times \mathbf{P}$.

Recall that in Section 3.1.2 we have seen that the position of the satellite in the perifocal frame is given by:

$$\mathbf{r}_{\text{Peri}} = a(\cos E - e)\mathbf{P} + a\sqrt{1-e^2}\sin E\mathbf{Q} \tag{64}$$

Differentiating yields:

$$\dot{\mathbf{r}}_{\text{Peri}} = -a(\sin E)\dot{E}\mathbf{P} + a\sqrt{1-e^2}(\cos E)\dot{E}\mathbf{Q} \tag{65}$$

where $\dot{E} = \frac{n}{1-e\cos E}$ is given by Eq. (35). These two quantities depend on the two unknown variables a and E, because n and e are given in the TLE data set. The semi-major axis can be easily obtained from n due to the Kepler's third law (Proposition 11). For the eccentric anomaly, we need to solve the Kepler equation:

$$E - e\sin E = M \tag{66}$$

Lemma 25. Let $e \in [0, 1)$ and $M \in \mathbb{R}$. Then, the function

$$f(E) = E - e\sin E - M \tag{67}$$

has a unique solution in the interval $[M, M + e]$.

Proof. We first prove the uniqueness. Clearly $f \in \mathcal{C}^1(\mathbb{R})$ and $f'(E) = 1 - e\cos E > 0$ for all $E \in [0, 2\pi)$ because $e < 1$. Thus, f is strictly increasing and so it has at most one zero. Now, let $\overline{M} := M \mod 2\pi \in [0, 2\pi)$. If $0 \leq \overline{M} < \pi$, then:

$$f(M) = -e\sin M \leq 0 \qquad \text{and} \qquad f(M+e) = e(1-\sin(M+e)) \geq 0 \tag{68}$$

So by Bolzano's theorem, f has a solution in $[M, M + e]$. If $\pi \leq \overline{M} < 2\pi$, then:

$$f(M) = -e\sin M \geq 0 \qquad \text{and} \qquad f(M-e) = -e(1+\sin(M-e)) \leq 0 \tag{69}$$

So again by Bolzano's theorem, f has a solution in $[M - e, M]$. □

We will use the Newton's method to find the zero of this non-linear equation. For small eccentricities e, the natural choice for the initial guess is $E_0 = M$. For large eccentricities ($e > 0.8$) the initial guess $E_0 = \pi$ should be used in order to avoid convergency problems [MG05]. Alternatively, we can do one or two steps of the bisection method to get a better initial guess, and then apply the Newton's method. Once obtained E, the position and velocity of the satellite in the J2000 frame are given by:

$$\mathbf{r}_{\text{ECI}} = \mathbf{T}\mathbf{r}_{\text{Peri}} \qquad \dot{\mathbf{r}}_{\text{ECI}} = \mathbf{T}\dot{\mathbf{r}}_{\text{Peri}} \tag{70}$$

where $\mathbf{T}$ is the rotation matrix that transforms one frame into the other and is given by (look at Fig. 16):

$$\mathbf{T} = \mathbf{R}_z(-\Omega)\mathbf{R}_x(-i)\mathbf{R}_z(-\omega) \tag{71}$$

4 Earth's gravitational field and other perturbations

So far we have only considered the gravitational force acting between point masses. In reality, the Earth is not a point mass, neither a spherically symmetric mass distribution. In this section we will delve into the details of a more realistic model of the Earth's gravitational field.

4.1 Geopotential model

4.1.1 Continuous distribution of mass

In Section 3.1 we saw that the motion of a body orbiting another one can be described by a conic section. However, we have not been concerned about the mass distribution of the large body, in our case the Earth. In this section we will see that the motion of the smaller body, the satellite, is slightly perturbed by the mass distribution of the Earth as well as the presence of other forces such as atmospheric drag, solar radiation pressure, or the gravitational pull of the Moon and Sun, which we will discuss later on. Nevertheless, the perturbations are relatively small and the orbits of the satellites are still approximating ellipses, but as we will corroborate experimentally in Section 5 these perturbations are essential to obtain accurate results.

Consider a body confined in a compact region $\Omega \subseteq \mathbb{R}$ with a continuous density of mass $\rho : \Omega \to \mathbb{R}$. We would like to know the gravitational pull on a point mass m located at position $\mathbf{r}$ from the center of mass of the body. To do this, consider a covering of Ω in a set of disjoint cubes Q_i, $i = 1, \dots, N$, small enough to be considered as point masses and let $R_i := Q_i \cap \Omega$. Then, $\bigsqcup_{i=1}^{N} R_i = \Omega$. If each R_i has mass m_i, volume V_i, density ρ_i, and its center is located at $\mathbf{s}_i \in \mathbb{R}^3$, then the total gravitational acceleration $\mathbf{g}$ exerted on m is the sum of the contributions of all the forces exerted by the N point masses, and it is given by:

$$\mathbf{g} = -\sum_{i=0}^{N} \frac{Gm_i}{\|\mathbf{r} - \mathbf{s}_i\|^3}(\mathbf{r} - \mathbf{s}_i) = -\sum_{i=0}^{N} \frac{G\rho_i}{\|\mathbf{r} - \mathbf{s}_i\|^3}(\mathbf{r} - \mathbf{s}_i)V_i \tag{72}$$

Note that Eq. (72) is a Riemann sum and so letting $N \to \infty$ we get:

$$\mathbf{g} = -\int_{\Omega} \frac{G\rho(\mathbf{s})}{\|\mathbf{r} - \mathbf{s}\|^3}(\mathbf{r} - \mathbf{s})\mathrm{d}^3\mathbf{s} \tag{73}$$

where $\mathrm{d}^3\mathbf{s} := \mathrm{d}x'\,\mathrm{d}y'\,\mathrm{d}z'$, if $\mathbf{s} = (x', y', z')$.

Theorem 26. Let Ω be a compact region in $\mathbb{R}^3$ with a continuous density of mass $\rho : \Omega \to \mathbb{R}$. Then, the gravitational acceleration field $\mathbf{g}$ is conservative. That is, there exists a function $V : \mathbb{R}^3 \to \mathbb{R}$ such that $\mathbf{g} = \boldsymbol{\nabla} V$. We call V the *gravitational potential*.

Proof. See **??**. □

Physically speaking, the gravitational force $\mathbf{F}$ being conservative means that the work W done by the force along a path C

$$W = \int_{C} \mathbf{F} \cdot \mathrm{d}\mathbf{s} \tag{74}$$

depends only on the initial and final positions of it.

4.1.2 Laplace's equation for V

Theorem 27. Consider a distribution of matter of density ρ in a compact region Ω. Then, the gravitational potential V satisfies the Laplace equation

$$\Delta V = 0 \tag{75}$$

for all points outside Ω[9].

[9] It can be seen that V satisfies in fact the *Poisson equation* $\Delta V = 4\pi G\rho$ for any point $\mathbf{r} \in \mathbb{R}^3$, which reduces to Laplace equation when $\mathbf{r} \in \Omega^c$, because there we have $\rho(\mathbf{r}) = 0$.

Proof. See **??**. □

So far we have seen that the gravitational potential V satisfies the Laplace equation. If, moreover, we choose the origin of potential to be at the infinity, that is, if we impose $\lim_{\|\mathbf{r}\|\to\infty} V = 0$, then the gravitational potential created by a distribution of mass in a compact region Ω is a solution of the following exterior Dirichlet problem:

$$\begin{cases} \Delta V = 0 & \text{in } \Omega^c \\ V = f & \text{on } \partial\Omega \\ \lim_{\|\mathbf{r}\|\to\infty} V = 0 \end{cases} \tag{76}$$

If Ω represents the Earth, then $f = f(\theta, \phi)$ is the boundary condition concerning the gravitational potential at the surface of the Earth as a function of the longitude θ and colatitude ϕ.

We will see now that Eq. (76) has a unique solution. To do that we invoke the maximum principle, which we will not prove here (see [Eva10] for more details).

Theorem 28 (Maximum principle). Let $U \subset \mathbb{R}^n$ be open and bounded and $u \in \mathcal{C}^2(U) \cap \mathcal{C}(\overline{U})$. Suppose that u is harmonic within U, that is, $\Delta u = 0$ in U. Then, $\max_{\overline{U}} u = \max_{\partial U} u$.

Theorem 29. The Dirichlet problem of Eq. (76) has a unique solution.

Proof. See **??**. □

Now that we know that the Dirichlet problem has a unique solution, we can proceed to find it. In the next section we will construct an explicit solution for the gravitational potential created by the Earth.

4.2 Spherical harmonics

4.2.1 Legendre polynomials, regularity and orthonormality

In this section we aim to introduce a class of functions that will appear later on in the general solution of the Laplace equation (see Section 4.2.2). To accomplish this, we need first to introduce the Legendre polynomials. There are several ways to define them, but the most convenient one for our purposes is from the following differential equation. Consider the following second-order differential equation called *Legendre differential equation*:

$$(1-x^2)y'' - 2xy' + \lambda y = 0 \tag{77}$$

for $\lambda \in \mathbb{R}$. This equation can be rewritten as:

$$\left((1-x^2)y'\right)' + \lambda y = 0 \tag{78}$$

Seeking for analytic solutions of this equation using the power series method [Mez], i.e. looking for solutions of the form $y(x) = \sum_{j=0}^{\infty} a_j x^j$, we see that:

$$\begin{aligned} 0 = (1-x^2)\sum_{j=2}^{\infty} a_j(j-1)jx^{j-2} - 2x\sum_{j=1}^{\infty} a_j j x^{j-1} + \lambda\sum_{j=0}^{\infty} a_j x^j = \sum_{j=0}^{\infty} a_{j+2}(j+1)(j+2)x^j - \\ - \sum_{j=0}^{\infty} a_j(j-1)jx^j - \sum_{j=0}^{\infty} 2a_j j x^j + \sum_{j=0}^{\infty} \lambda a_j x^j = \sum_{j=0}^{\infty} [a_{j+2}(j+1)(j+2) - a_j(j(j+1)-\lambda)]x^j \end{aligned} \tag{79}$$

Equating the general term of the series to 0 we obtain this recursion:

$$a_{j+2} = \frac{j(j+1)-\lambda}{(j+1)(j+2)} a_j \quad j = 0, 1, 2, \ldots \tag{80}$$

From here we can obtain two independent solutions by setting the initial conditions a_0 and a_1 of the iteration. For example, setting $a_1 = 0$ we obtain a series that has only even powers of x. On the other hand, setting $a_0 = 0$ we obtain a series that has only odd powers of x. These two series converge on the interval $(-1, 1)$ by the ratio test (by looking at Eq. (80)) and can be expressed compactly as [Mez]:

$$y_{\mathrm{e}}(x) = a_0 \sum_{j=0}^{\infty} \left[\prod_{k=0}^{j-1}(2k(2k+1)-\lambda)\right] \frac{x^{2j}}{(2j)!} \quad y_{\mathrm{o}}(x) = a_1 \sum_{j=0}^{\infty} \left[\prod_{k=0}^{j-1}((2k+1)(2k+2)-\lambda)\right] \frac{x^{2j+1}}{(2j+1)!} \tag{81}$$

Here, the empty product (that is, when k ranges from 0 to -1) is defined to be 1. However, for each $\lambda \in \mathbb{R}$ either one of these series or both diverge at $x = \pm 1$, as they behave as the harmonic series in a neighborhood of $x = \pm 1$. We are interested, though, in the solutions that remain bounded on the whole interval $[-1, 1]$. Looking at the expressions of Eq. (81) one can check that the only possibility to make the series converge in $[-1, 1]$ is when $\lambda = n(n+1)$, $n \in \mathbb{N} \cup \{0\}$. In this case, for each $n \in \mathbb{N} \cup \{0\}$ exactly one of the series is in fact a polynomial of degree n. If, furthermore, we choose a_0 or a_1 be such that the polynomial evaluates to 1 at $x = 1$, these polynomials are called *Legendre polynomials*, and they are denoted by $P_n(x)$. The other (divergent) series is usually denoted in the literature by $Q_n(x)$ (check [RHB99; Mez]) and it is independent of $P_n(x)$. Thus, the general solution of Eq. (78) for $\lambda = n(n+1)$ can be expressed as a linear combination of P_n and Q_n, because the space of solutions form a vector space of dimension 2.

n	$P_n(x)$
0	1
1	x
2	$\frac{1}{2}(3x^2 - 1)$
3	$\frac{1}{2}(5x^3 - 3x)$
4	$\frac{1}{8}(35x^4 - 30x^2 + 3)$
5	$\frac{1}{8}(63x^5 - 70x^3 + 15x)$
6	$\frac{1}{16}(231x^6 - 315x^4 + 105x^2 - 5)$
7	$\frac{1}{16}(429x^7 - 693x^5 + 315x^3 - 35x)$

Table 3: First eight Legendre polynomials

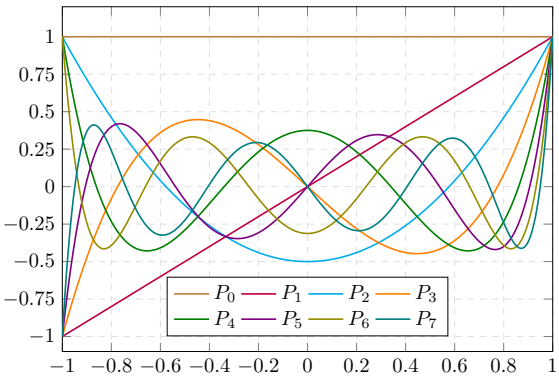

Figure 17: Graphic representation of the first eight Legendre polynomials.

The following proposition will be of our interest in the next section [RHB99].

Proposition 30. Let $y(x)$ be a solution to the Legendre differential equation. Then, $\forall m \in \mathbb{N} \cup \{0\}$ the function

$$w_m(x) = (1 - x^2)^{m/2} \frac{\mathrm{d}^m y(x)}{\mathrm{d}x^m} \tag{82}$$

solves the *general Legendre differential equation*:

$$(1 - x^2)y'' - 2xy' + \left(\lambda - \frac{m^2}{1 - x^2}\right) y = 0 \tag{83}$$

In particular if $\lambda = n(n+1)$ for $n \in \mathbb{N} \cup \{0\}$, then $w_m(x)$ is denoted as

$$P_{n,m}(x) := (1 - x^2)^{m/2} \frac{\mathrm{d}^m P_n}{\mathrm{d}x^m} \tag{84}$$

and it is called the *associated Legendre polynomial* of degree n and order m.

Note that although we opted to call the functions $P_{n,m}$ as polynomials, they are only true polynomials when m is even. But we have opted to call them in that manner as it is the common practice in the literature (see [Wei; RHB99; Mez]).

Moreover, from the definition of $P_{n,m}$, we can see that $P_{n,0} = P_n$ and that $P_{n,m} = 0$ if $m > n$. So we can restrict the domain of m to the set $\{0, 1, \ldots, n\}$.

n	$P_{n,1}(x)$	n	$P_{n,2}(x)$
1	$\sqrt{1 - x^2}$	2	$3(1 - x^2)$
2	$3x\sqrt{1 - x^2}$	3	$15x(1 - x^2)$
3	$\frac{3}{2}(5x^2 - 1)\sqrt{1 - x^2}$	4	$\frac{15}{2}(7x^2 - 1)(1 - x^2)$
4	$\frac{5}{2}x(7x^2 - 3)\sqrt{1 - x^2}$	5	$\frac{105}{2}x(3x^2 - 1)(1 - x^2)$
5	$\frac{15}{8}(21x^4 - 14x^2 + 1)\sqrt{1 - x^2}$	6	$\frac{105}{8}(33x^4 - 18x^2 + 1)(1 - x^2)$

Table 4: First associated Legendre polynomials for $m = 1$ and $m = 2$.

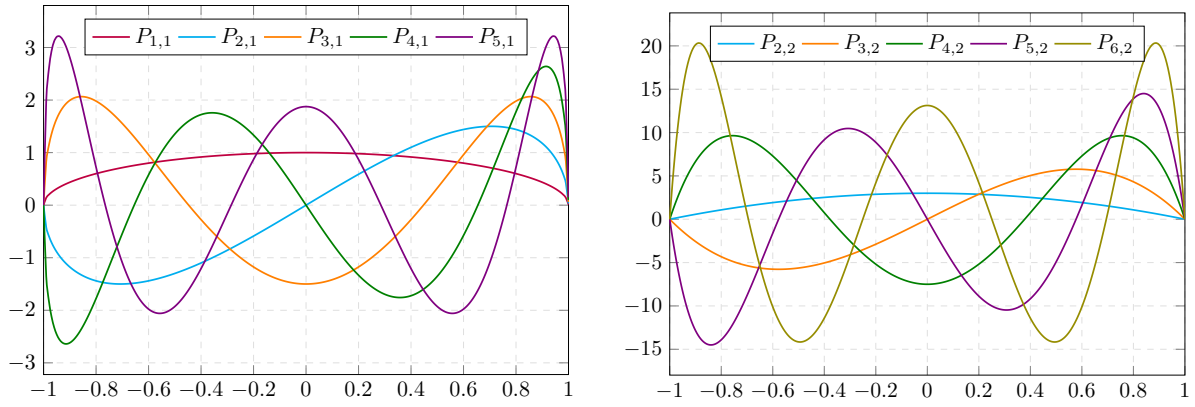

(a) $m = 1$ **(b)** $m = 2$

Figure 18: Graphic representation of the first associated Legendre polynomials for $m = 1$ and $m = 2$.

Definition 31. Let $n \in \mathbb{N} \cup \{0\}$ and $m \in \{0, 1, \dots, n\}$. We define the *real spherical harmonics* $Y^{\mathrm{c}}_{n,m}$ and $Y^{\mathrm{s}}_{n,m}$ as:

$$Y^{\mathrm{c}}_{n,m}(\theta, \phi) = \sqrt{(2 - \delta_{0,m})(2n + 1)\frac{(n - m)!}{(n + m)!}} P_{n,m}(\cos\phi) \cos m\theta \tag{85}$$

$$Y^{\mathrm{s}}_{n,m}(\theta, \phi) = \sqrt{(2 - \delta_{0,m})(2n + 1)\frac{(n - m)!}{(n + m)!}} P_{n,m}(\cos\phi) \sin m\theta \tag{86}$$

Here the coordinates $\theta \in [0, 2\pi)$ and $\phi \in [0, \pi]$ are the spherical coordinates such that any point on the sphere can be written uniquely as $(x, y, z) = (\sin\phi\cos\theta, \sin\phi\sin\theta, \cos\phi)$. The factor $N_{n,m} := \sqrt{(2 - \delta_{0,m})(2n + 1)\frac{(n-m)!}{(n+m)!}}$ is called the *normalization factor* of the spherical harmonics and $\delta_{0,m}$ is the Kronecker delta and their appearance here will become clear in the next section.

n	m	$Y^{\mathrm{c}}_{n,m}(\theta, \phi)$	n	m	$Y^{\mathrm{c}}_{n,m}(\theta, \phi)$
0	0	1	2	2	$\frac{\sqrt{15}}{2}(\sin\phi)^2 \cos 2\theta$
1	0	$\sqrt{3}\cos\phi$	3	0	$\frac{\sqrt{7}}{2}\cos\phi(5(\cos\phi)^2 - 3)$
1	1	$\sqrt{3}\sin\phi\cos\theta$	3	1	$\frac{\sqrt{42}}{4}(5(\cos\phi)^2 - 1)\sin\phi\cos\theta$
2	0	$\frac{\sqrt{5}}{2}(3(\cos\phi)^2 - 1)$	3	2	$\frac{\sqrt{105}}{2}(\sin\phi)^2\cos\phi\cos 2\theta$
2	1	$\sqrt{15}\sin\phi\cos\phi\cos\theta$	3	3	$\frac{\sqrt{70}}{4}(\sin\phi)^3\cos 3\theta$

Table 5: First cosine spherical harmonics.

The associated Legendre polynomials satisfy an orthogonality relation:

Lemma 32. Let $n_1, n_2 \in \mathbb{N} \cup \{0\}$ and $m \leq \min\{n_1, n_2\}$. Then:

$$\int_0^1 P_{n_1,m}(x) P_{n_2,m}(x)\,\mathrm{d}x = \frac{2}{2n_1 + 1}\frac{(n_1 + m)!}{(n_1 - m)!}\delta_{n_1,n_2} \tag{87}$$

where δ_{n_1,n_2} denotes the Kronecker delta.

Similarly, it can be shown that the spherical harmonics from an orthonormal family of functions:

Proposition 33. The family of spherical harmonics $\{Y^{\mathrm{c}}_{n,m}(\theta, \phi), Y^{\mathrm{s}}_{n,m}(\theta, \phi) : n \in \mathbb{N} \cup \{0\}, m \leq n\}$ is orthonormal in the following sense:

$$\frac{1}{4\pi}\int_0^{2\pi}\int_0^{\pi} Y^i_{n_1,m_1}(\theta, \phi) Y^j_{n_2,m_2}(\theta, \phi)\mathrm{d}\Omega = \delta_{n_1,n_2}\delta_{m_1,m_2}\delta_{i,j} \tag{88}$$

where $\mathrm{d}\Omega = \sin\phi\,\mathrm{d}\phi\,\mathrm{d}\theta$ is the solid angle element, which measures the element of area on a sphere of radius 1.

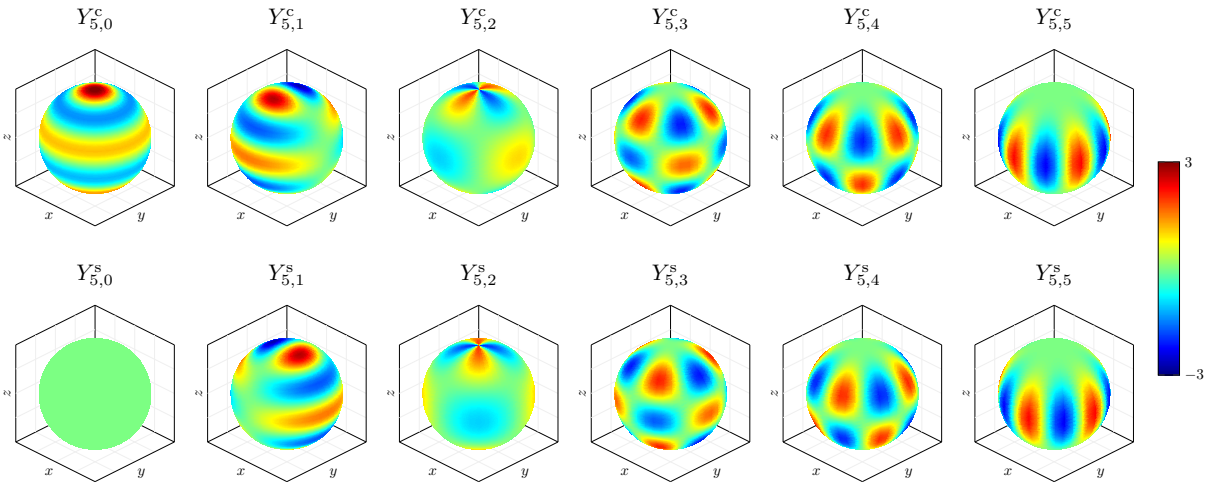

Figure 19: 3D color gradient representation of the spherical harmonics of degree $n = 5$. The first row correspond to the cosine spherical harmonics and the second row correspond to the sine spherical harmonics.

Proof. See **??**. □

Moreover, an important result in the Sturm-Liouville Theory of second order differential equations ([Wikd; Wan+09]) says that the family of spherical harmonics $\{Y^{c}_{n,m}(\theta,\phi), Y^{s}_{n,m}(\theta,\phi) : n \in \mathbb{N}\cup\{0\}, m \leq n\}$ form a complete set in the sense that any smooth function defined on the sphere $f : \mathrm{S}^2 \to \mathbb{R}$ can be expanded in a series of spherical harmonics:

$$f(\theta,\phi) = \sum_{n=0}^{\infty}\sum_{m=0}^{n}\left(c_{n,m}Y^{c}_{n,m}(\theta,\phi) + s_{n,m}Y^{s}_{n,m}(\theta,\phi)\right) \tag{89}$$

This will be useful in Section 4.2.3 when expanding the gravitational potential created by the Earth at some arbitrary point in spherical harmonics.

4.2.2 Laplace's equation in spherical coordinates

We start first with this proposition that give us the laplacian of a function in spherical coordinates.

Proposition 34. Let $f : \mathbb{R}^3 \to \mathbb{R}$ be a twice-differentiable function. Then:

$$\Delta f = \frac{1}{r^2}\frac{\partial}{\partial r}\left(r^2\frac{\partial f}{\partial r}\right) + \frac{1}{r^2\sin\phi}\frac{\partial}{\partial\phi}\left(\sin\phi\frac{\partial f}{\partial\phi}\right) + \frac{1}{r^2(\sin\phi)^2}\frac{\partial^2 f}{\partial\theta^2} \tag{90}$$

where $r \in [0,\infty)$ denotes the radial distance, $\theta \in [-\pi,\pi)$ denotes the longitude, and $\phi \in [0,\pi]$, the colatitude:

$$\begin{aligned} x &= r\sin\phi\cos\theta \\ y &= r\sin\phi\sin\theta \\ z &= r\cos\phi \end{aligned} \tag{91}$$

We are now interested in solving the Laplace equation. Theorem 35 gives the solution of it as a function of the spherical harmonics.

Theorem 35. The regular solutions in a bounded region $\Omega \subseteq \mathbb{R}^3$ such that $0 \notin \overline{\Omega}$ of the Laplace equation in spherical coordinates are of the form

$$f(r,\theta,\phi) = \sum_{n=0}^{\infty}\sum_{m=0}^{n}(a_n r^n + b_n r^{-n-1})P_{n,m}(\cos\phi)(c_{n,m}\cos(m\theta) + s_{n,m}\sin(m\theta)) \tag{92}$$

$$= \sum_{n=0}^{\infty}\sum_{m=0}^{n}(a_n r^n + b_n r^{-n-1})(\tilde{c}_{n,m}Y^{c}_{n,m}(\theta,\phi) + \tilde{s}_{n,m}Y^{s}_{n,m}(\theta,\phi)) \tag{93}$$

where $a_n, b_n, c_{n,m}, s_{n,m}, \tilde{c}_{n,m}, \tilde{s}_{n,m} \in \mathbb{R}$.

Proof. See **??**. □

We ignore the singularity at $r = 0$ of Eq. (93) from now. In the next section we discuss it in more detail.

4.2.3 Expansion in spherical harmonics

We have just seen that if V satisfies the exterior Dirichlet problem for the Laplace equation, then, by uniqueness of solutions, it can be expressed as:

$$V(r,\theta,\phi) = \sum_{n=0}^{\infty}\sum_{m=0}^{n}(a_n r^n + b_n r^{-n-1})(\tilde{c}_{n,m}Y^{\mathrm{c}}_{n,m}(\theta,\phi) + \tilde{s}_{n,m}Y^{\mathrm{s}}_{n,m}(\theta,\phi)) \tag{94}$$

for some $a_n, b_n, \tilde{c}_{n,m}, \tilde{s}_{n,m} \in \mathbb{R}$. If we impose V to satisfy the third condition of Eq. (76), we must have $a_n = 0$. Finally, if we choose $R_\oplus$ as a reference radius for a spherical model of the Earth, using the boundary condition on $\partial\,\Omega$

$$f(\theta,\phi) = \sum_{n=0}^{\infty}\sum_{m=-n}^{n}\frac{b_n}{{R_\oplus}^{n+1}}(\tilde{c}_{n,m}Y^{\mathrm{c}}_{n,m}(\theta,\phi) + \tilde{s}_{n,m}Y^{\mathrm{s}}_{n,m}(\theta,\phi)) \tag{95}$$

and the orthogonality of the spherical harmonics, we can deduce that the coefficients $b_n\tilde{c}_{n,m}$ and $b_n\tilde{s}_{n,m}$ are given by:

$$b_n\tilde{c}_{n,m} = \frac{{R_\oplus}^{n+1}}{4\pi}\int_0^{2\pi}\int_0^{\pi} f(\theta,\phi)Y^{\mathrm{c}}_{n,m}(\theta,\phi)\sin\phi\,\mathrm{d}\phi\,\mathrm{d}\theta \tag{96}$$

$$b_n\tilde{s}_{n,m} = \frac{{R_\oplus}^{n+1}}{4\pi}\int_0^{2\pi}\int_0^{\pi} f(\theta,\phi)Y^{\mathrm{s}}_{n,m}(\theta,\phi)\sin\phi\,\mathrm{d}\phi\,\mathrm{d}\theta \tag{97}$$

Hence, introducing the gravitational constant G and the Earth's mass $M_\oplus$ into the equation, our final expression for the gravitational potential is

$$V(r,\theta,\phi) = \frac{GM_\oplus}{R_\oplus}\sum_{n=0}^{\infty}\sum_{m=0}^{n}\left(\frac{R_\oplus}{r}\right)^{n+1}(\bar{C}_{n,m}Y^{\mathrm{c}}_{n,m}(\theta,\phi) + \bar{S}_{n,m}Y^{\mathrm{s}}_{n,m}(\theta,\phi)) \tag{98}$$

where the coefficients $\bar{C}_{n,m}, \bar{S}_{n,m} \in \mathbb{R}$ are given by the formulas:

$$\bar{C}_{n,m} = \frac{1}{4\pi}\frac{R_\oplus}{GM_\oplus}\int_0^{2\pi}\int_0^{\pi} f(\theta,\phi)Y^{\mathrm{c}}_{n,m}(\theta,\phi)\sin\phi\,\mathrm{d}\phi\,\mathrm{d}\theta \tag{99}$$

$$\bar{S}_{n,m} = \frac{1}{4\pi}\frac{R_\oplus}{GM_\oplus}\int_0^{2\pi}\int_0^{\pi} f(\theta,\phi)Y^{\mathrm{s}}_{n,m}(\theta,\phi)\sin\phi\,\mathrm{d}\phi\,\mathrm{d}\theta \tag{100}$$

The coefficients $\bar{C}_{n,m}$, $\bar{S}_{n,m}$ are called *geopotential coefficients*, and they describe the dependence on the Earth's internal structure. They are obtained from observation of the perturbations seen in the orbits of other satellites [MG05], because it is not possible to measure the Earth's density directly. Other methods for obtaining such data are through surface gravimetry, which provides precise local and regional information about the gravity field, or through altimeter data, which can be used to provide a model for the geoid of the Earth (which is the shape that the ocean surface takes under the influence of the gravity of Earth) which in turn can be used to obtain the geopotential coefficients.

4.3 Numerical computation

4.3.1 Gravitational acceleration

Up to this point, we have only studied the gravitational potential exerted by the non-homogeneous Earth on a satellite. But, in order to integrate the equations of motion of the satellite, we need to compute

the gravitational acceleration $\mathbf{g} = -\boldsymbol{\nabla} V$ instead. In order to do this efficiently, we will make use of the following formulas given in [MG05; Cun70]. First, let

$$V_{n,m}(\theta,\phi) = \left(\frac{R_\oplus}{r}\right)^{n+1} P_{n,m}(\cos\phi)\cos(m\theta) \qquad W_{n,m}(\theta,\phi) = \left(\frac{R_\oplus}{r}\right)^{n+1} P_{n,m}(\cos\phi)\sin(m\theta) \tag{101}$$

Thus, we can write:

$$V = \frac{GM_\oplus}{R_\oplus}\sum_{n=0}^{\infty}\sum_{m=0}^{n}(\bar{C}_{n,m}N_{n,m}V_{n,m} + \bar{S}_{n,m}N_{n,m}W_{n,m}) \tag{102}$$

Let $C_{n,m} := \bar{C}_{n,m}N_{n,m}$ and $S_{n,m} := \bar{S}_{n,m}N_{n,m}$. If $\mathbf{g} = (\ddot{x}, \ddot{y}, \ddot{z})$, then:

$$\ddot{x} = \sum_{n=0}^{\infty}\sum_{m=0}^{n}\ddot{x}_{n,m} \qquad \ddot{y} = \sum_{n=0}^{\infty}\sum_{m=0}^{n}\ddot{y}_{n,m} \qquad \ddot{z} = \sum_{n=0}^{\infty}\sum_{m=0}^{n}\ddot{z}_{n,m} \tag{103}$$

where the *partial* accelerations $\ddot{x}_{n,m}$, $\ddot{y}_{n,m}$, $\ddot{z}_{n,m}$ are given by:

$$\ddot{x}_{n,m} = \begin{cases} -\dfrac{GM_\oplus}{{R_\oplus}^2}C_{n,0}V_{n+1,1} & \text{if } m = 0 \\ -\dfrac{GM_\oplus}{{R_\oplus}^2}\cdot\dfrac{1}{2}\Big[C_{n,m}V_{n+1,m+1} + S_{n,m}W_{n+1,m+1} - \\ \qquad -\dfrac{(n-m+2)!}{(n-m)!}\left(C_{n,m}V_{n+1,m-1} + S_{n,m}W_{n+1,m-1}\right)\Big] & \text{if } m > 0 \end{cases} \tag{104}$$

$$\ddot{y}_{n,m} = \begin{cases} -\dfrac{GM_\oplus}{{R_\oplus}^2}C_{n,0}W_{n+1,1} & \text{if } m = 0 \\ -\dfrac{GM_\oplus}{{R_\oplus}^2}\cdot\dfrac{1}{2}\Big[C_{n,m}W_{n+1,m+1} - S_{n,m}V_{n+1,m+1} - \\ \qquad -\dfrac{(n-m+2)!}{(n-m)!}\left(C_{n,m}W_{n+1,m-1} - S_{n,m}V_{n+1,m-1}\right)\Big] & \text{if } m > 0 \end{cases} \tag{105}$$

$$\ddot{z}_{n,m} = -\frac{GM_\oplus}{{R_\oplus}^2}(n-m+1)\left(C_{n,m}V_{n+1,m} + S_{n,m}W_{n+1,m}\right) \tag{106}$$

and the functions $V_{n,m}$, $W_{n,m}$ are calculated using the following recurrence relations:

$$\begin{cases} V_{n,m} = \dfrac{2n-1}{n-m}\dfrac{R_\oplus}{r}\cos\phi V_{n-1,m} - \dfrac{n+m-1}{n-m}\dfrac{{R_\oplus}^2}{r^2}V_{n-2,m} \\ W_{n,m} = \dfrac{2n-1}{n-m}\dfrac{R_\oplus}{r}\cos\phi W_{n-1,m} - \dfrac{n+m-1}{n-m}\dfrac{{R_\oplus}^2}{r^2}W_{n-2,m} \end{cases} \quad \text{if } 0 \le m \le n-2$$

$$\begin{cases} V_{n,n-1} = (2n-1)\dfrac{R_\oplus}{r}\cos\phi V_{n-1,n-1} \\ W_{n,n-1} = (2n-1)\dfrac{R_\oplus}{r}\cos\phi W_{n-1,n-1} \end{cases} \quad \text{if } m = n-1 \tag{107}$$

$$\begin{cases} V_{n,n} = (2m-1)\dfrac{R_\oplus}{r}\sin\phi[\cos\theta V_{n-1,n-1} - \sin\theta W_{n-1,n-1}] \\ W_{n,n} = (2m-1)\dfrac{R_\oplus}{r}\sin\phi[\cos\theta W_{n-1,n-1} + \sin\theta V_{n-1,n-1}] \end{cases} \quad \text{if } m = n$$

starting from the initial quantities $V_{00} = \frac{R_\oplus}{r}$ and $W_{00} = 0$ and using the scheme of Fig. 20 [MG05].

4.4 Other perturbations

So far we have only considered one force acting on the satellite: the gravitational force exerted by the Earth. However, there are other important forces worth-considering, and they relative importance varies depending on the satellite's altitude.

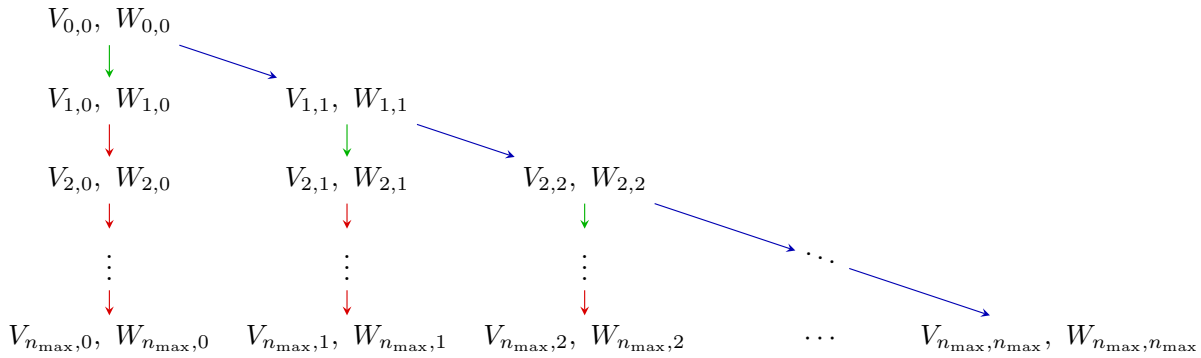

Figure 20: Scheme for the calculation of the coefficients $V_{n,m}$ and $W_{n,m}$ for $0 \leq m \leq n \leq n_{\max}$. The red arrows indicate that the coefficients are calculated using the first of the above recursions; the green arrows indicate that they are calculated using the second recursion; and the blue arrows indicate that they are calculated using the third recursion.

4.4.1 Atmospheric drag

For *LEO* (*Low Earth Orbit*) satellites, that is, satellites with an altitude of less than 1 000 km, the most important perturbation is the atmospheric drag. Indeed, as these satellites travel in the upper layers of the atmosphere, they are subject to a drag force caused by the interaction with air particles. The acceleration due to drag can be written as:

$$\mathbf{a}_{\mathrm{D}} = -\frac{1}{2} C_{\mathrm{D}} \frac{A}{m} \rho v_{\mathrm{rel}} \mathbf{v}_{\mathrm{rel}} \tag{108}$$

where A is the cross-sectional area of the satellite, m is its mass, ρ is the atmospheric density, $\mathbf{v}_{\mathrm{rel}}$ is the relative velocity between the satellite and the air particles, $v_{\mathrm{rel}} = \|\mathbf{v}_{\mathrm{rel}}\|$, and C_{D} is the drag coefficient, which depends on the shape of the satellite and the properties of the air particles. In order to determine $\mathbf{v}_{\mathrm{rel}}$, we will suppose that the atmospheric particles rotate with the Earth, and thus the relative velocity is given by:

$$\mathbf{v}_{\mathrm{rel}} = \dot{\mathbf{r}} - \boldsymbol{\omega}_{\oplus} \times \mathbf{r} \tag{109}$$

where $\boldsymbol{\omega}_{\oplus}$ is the angular velocity of the Earth.

The complexity of modeling this force arises from the challenge of representing accurately the atmospheric density as a function of the altitude. We will not delve into this topic, but in the simulation we will use the density model of Harris-Priester, which is valid for altitudes between 100 and 1 000 km (see [MG05] for more details).

4.4.2 Sun and Moon gravitational perturbations

For *MEO* (*Medium Earth Orbit*) satellites, within an altitude between 1 000 and 35 780 km [Val13]; *GEO* (*Geostationary Earth Orbit* or *Geosynchronous Earth Orbit*) satellites, with an altitude of around 35 780 km; and *HEO* (*High Earth Orbit*) satellites, with an altitude of more than 35 780 km, the most important perturbations are the gravitational perturbations caused by the Moon and the Sun, or even other celestial bodies.

Adding a third body into the equations requires some carefulness. We will do the general deduction to make it clear for the reader. Suppose we have $N+2$ bodies of masses M, $M_1, \ldots, M_N$ and $m \ll M, M_1, \ldots, M_N$ at positions $\mathbf{s}$, $\mathbf{s}_1, \ldots, \mathbf{s}_N$ and $\mathbf{r}$, respectively, in an inertial reference frame (we omit the dependence in time). The dynamics of this system are governed by the following system of differential equations:

$$\begin{cases} \ddot{\mathbf{s}} = \displaystyle\sum_{i=1}^{N} \frac{GM_i}{\|\mathbf{s}_i - \mathbf{s}\|^3}(\mathbf{s}_i - \mathbf{s}) + \frac{Gm}{\|\mathbf{r} - \mathbf{s}\|^3}(\mathbf{r} - \mathbf{s}) \\ \ddot{\mathbf{s}}_i = \dfrac{GM}{\|\mathbf{s} - \mathbf{s}_i\|^3}(\mathbf{s} - \mathbf{s}_i) + \displaystyle\sum_{\substack{j=1 \\ j \neq i}}^{N} \frac{GM_j}{\|\mathbf{s}_j - \mathbf{s}_i\|^3}(\mathbf{s}_j - \mathbf{s}_i) + \frac{Gm}{\|\mathbf{r} - \mathbf{s}_i\|^3}(\mathbf{r} - \mathbf{s}_i) \quad \text{for } i = 1, \ldots, N \\ \ddot{\mathbf{r}} = \dfrac{GM}{\|\mathbf{s} - \mathbf{r}\|^3}(\mathbf{s} - \mathbf{r}) + \displaystyle\sum_{i=1}^{N} \frac{GM_i}{\|\mathbf{s}_i - \mathbf{r}\|^3}(\mathbf{s}_i - \mathbf{r}) \end{cases} \tag{110}$$

Here G is the gravitational constant. Since $m \ll M, M_1, \ldots, M_N$, we can assume that the motion of the large bodies is not affected by the small body, i.e. we can make m tend to zero and assume:

$$\begin{cases} \ddot{\mathbf{s}} = \displaystyle\sum_{i=1}^{N} \frac{GM_i}{\|\mathbf{s}_i - \mathbf{s}\|^3}(\mathbf{s}_i - \mathbf{s}) \\ \ddot{\mathbf{s}}_i = \dfrac{GM}{\|\mathbf{s} - \mathbf{s}_i\|^3}(\mathbf{s} - \mathbf{s}_i) + \displaystyle\sum_{\substack{j=1 \\ j\neq i}}^{N} \frac{GM_j}{\|\mathbf{s}_j - \mathbf{s}_i\|^3}(\mathbf{s}_j - \mathbf{s}_i) \quad \text{for } i = 1, \ldots, N \\ \ddot{\mathbf{r}} = \dfrac{GM}{\|\mathbf{s} - \mathbf{r}\|^3}(\mathbf{s} - \mathbf{r}) + \displaystyle\sum_{i=1}^{N} \frac{GM_i}{\|\mathbf{s}_i - \mathbf{r}\|^3}(\mathbf{s}_i - \mathbf{r}) \end{cases} \tag{111}$$

For our purposes, if the body of mass M is the Earth and the body of mass m is the satellite, we are interested in the position of the satellite relative to the Earth, that is $\mathbf{R} = \mathbf{r} - \mathbf{s}$. The dynamics of $\mathbf{R}$ is governed by the following equation:

$$\ddot{\mathbf{R}} = -\frac{GM}{\|\mathbf{R}\|^3}\mathbf{R} + \sum_{i=1}^{N} \frac{GM_i}{\|\mathbf{s}_i - \mathbf{s} - \mathbf{R}\|^3}(\mathbf{s}_i - \mathbf{s} - \mathbf{R}) - \sum_{i=1}^{N} \frac{GM_i}{\|\mathbf{s}_i - \mathbf{s}\|^3}(\mathbf{s}_i - \mathbf{s}) \tag{112}$$

Taking the origin of the inertial reference frame at the center of mass of the Earth, i.e. $\mathbf{s} = 0$, the latter equation finally becomes:

$$\ddot{\mathbf{R}} = -\frac{GM}{\|\mathbf{R}\|^3}\mathbf{R} + \sum_{i=1}^{N} \frac{GM_i}{\|\mathbf{s}_i - \mathbf{R}\|^3}(\mathbf{s}_i - \mathbf{R}) - \sum_{i=1}^{N} \frac{GM_i}{\|\mathbf{s}_i\|^3}\mathbf{s}_i = -\frac{GM}{\|\mathbf{R}\|^3}\mathbf{R} + \sum_{i=1}^{N} \mathbf{a}_i \tag{113}$$

where $\mathbf{a}_i = \frac{GM_i}{\|\mathbf{s}_i - \mathbf{R}\|^3}(\mathbf{s}_i - \mathbf{R}) - \frac{GM_i}{\|\mathbf{s}_i\|^3}\mathbf{s}_i$ is the contribution of the i-th body to the acceleration of the satellite. In the simulation, we will replace the first term of the right-hand side of the equation by the expansion of the acceleration in spherical harmonics.

4.4.3 Solar radiation pressure

Satellites in medium and high-altitude orbits may also experience a force that arises from the absortion or reflection of photons emitted by the Sun [MG05]. We will expose a brief overview on how this solar radiation pressure is modeled and how it is included in the equations of motion. The acceleration due to solar radiation pressure is given by:

$$\mathbf{a}_{\mathrm{R}} = -P_{\odot} C_{\mathrm{R}} \frac{A_{\odot}}{m} \frac{\mathbf{s}_{\odot} - \mathbf{r}}{\|\mathbf{s}_{\odot} - \mathbf{r}\|} \tag{114}$$

Here $P_{\odot} = 4.57 \times 10^{-6}$ N/m^2 is the solar radiation pressure at around the distance of the Earth, $C_{\mathrm{R}} = 1 + \varepsilon \in [0, 2]$ is the radiation pressure coefficient and ε is the reflectivity coefficient, being $C_{\mathrm{R}} = 0$ for a perfectly translucent body, $C_{\mathrm{R}} = 1$ for a perfectly absorbing body, and $C_{\mathrm{R}} = 2$ for a perfectly reflecting body. $\mathbf{r}$ denotes the position of the satellite relative to the Earth, $\mathbf{s}_{\odot}$ is the position of the Sun relative to the Earth, m the mass of the satellite and $A_{\odot}$ its fraction of area exposed to the Sun.

One should note that $A_{\odot}$ and A (the cross-sectional area of the satellite used to compute the drag force) are in general not the same. We will see in the next section, though, that due to the difficulties on determining them, we will assume that they are equal and constant throughout the integration process.

In reality, Eq. (114) does not describe entirely well the perturbation due to the solar radiation. Indeed, an illumination factor $\nu \in [0, 1]$ should be added into the equation to account for the fraction of solar rays that actually reach the satellite. This cause the disctinction of three regions: the illumination zone ($\nu = 1$), where the satellite is fully exposed to the Sun; the penumbral zone ($0 < \nu < 1$), where the satellite is partially exposed to the Sun, and the umbral zone ($\nu = 0$), where the satellite receives no solar radiation due to the Earth obstructing the light. Thus, Eq. (114) should be corrected to:

$$\mathbf{a}_{\mathrm{R}} = -\nu P_{\odot} C_{\mathrm{R}} \frac{A_{\odot}}{m} \frac{\mathbf{s}_{\odot} - \mathbf{r}}{\|\mathbf{s}_{\odot} - \mathbf{r}\|^3} \tag{115}$$

Fig. 21 shows a 2D schematic representation of the penumbra and umbral zones of the Earth. To determine whether the satellite is or not inside on of these zones, we must compute the dot product between $\mathbf{r}$ and $\mathbf{s}_{\odot}$ and if it is negative, then compare the relative "altitude" of the satellite with respect to the "altitudes" of the penumbral and umbral zones (y_{sat}, y_{pen} and y_{umb} respectively in the figure).

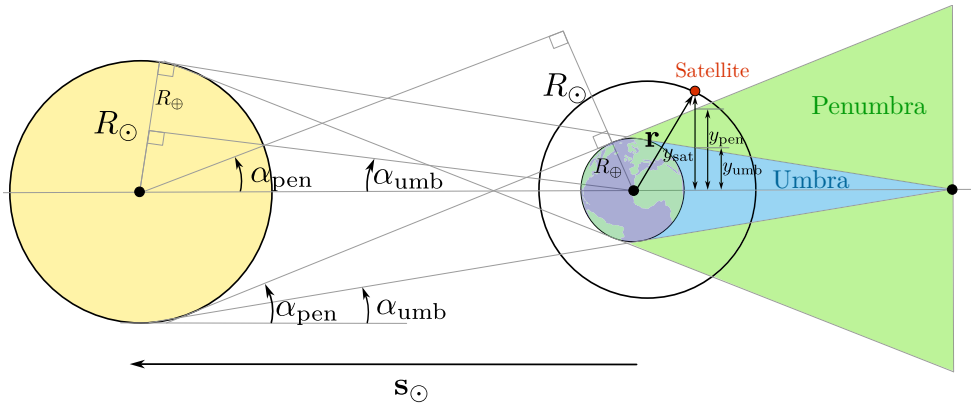

Figure 21: Schematic representation of the penumbra and umbral zones. Based on [Val13].

4.4.4 Minor perturbations

In addition to the major perturbations described above, there are other minor perturbations that we will not consider in this work, but they are worth-considering if accurate results are required. Some of these perturbations include the perturbations caused by other planets, relativistic effects, the Earth tide effects, or radiation pressure caused by the sunlight reflected by the Earth (albedo) [MG05].

5 Simulation

5.1 Introduction

Now, with all the ingredients in place, we can proceed to simulate the propagation of trajectories of some satellites. Summarizing all the perturbations considered in this project, we have that the position $\mathbf{r}$ and velocity $\mathbf{v} = \dot{\mathbf{r}}$ of the satellite will be governed by the following system of differential equations:

$$\begin{cases} \dot{\mathbf{r}} = \mathbf{v} \\ \dot{\mathbf{v}} = \mathbf{a}_{\text{GP}} + \delta_{\text{D}}\mathbf{a}_{\text{D}} + \delta_{\text{R}}\mathbf{a}_{\text{R}} + \delta_{\text{sun}}\mathbf{a}_{\text{sun}} + \delta_{\text{moon}}\mathbf{a}_{\text{moon}} \end{cases} \tag{116}$$

where $\mathbf{a}_{\text{GP}} = (\ddot{x}, \ddot{y}, \ddot{z})$ is the acceleration caused by the geopotential and $\ddot{x}$, $\ddot{y}$ and $\ddot{z}$ are given in Eq. (103); $\mathbf{a}_{\text{D}}$ is the acceleration caused by the atmospheric drag; $\mathbf{a}_{\text{R}}$ is the acceleration caused by the solar radiation pressure; $\mathbf{a}_{\text{sun}}$ is the acceleration caused by the Sun; and $\mathbf{a}_{\text{moon}}$ is the acceleration caused by the Moon. The coefficients $\delta_i \in \{0, 1\}$ are used to enable and disable the different perturbations. The initial conditions of the initial value problem will be the position and velocity obtained from the TLE. In order to solve this system of 6 differential equations, we have opted to use the Runge-Kutta-Fehlberg method of order 7(8) with a relative tolerance of 10^{-12} and using the SI units for the integration[10]. For the computation of the geopotential acceleration we will use the recursions of Eqs. (104) to (106) until $n = 8$.

There is, however, a significant comment to be made. In reality, the TLE sets are generated using a *Simplified General Perturbations* (*SGP*) model, and the data stored in the TLE does not contain the instantaneous orbital elements of the satellite, but doubly-averaged mean elements calculated to fit a set of observations [Kel; Val+06; VC08]. They are created with the SGP4 model[11] and, thus, we will use this software in order to obtain the position and velocity of each TLE.

That being said, we can proceed to show the results. We have chosen to simulate the propagation of the trajectories of satellites from very different altitudes: LEO satellites, MEO satellites and GEO satellites. Fig. 22 shows a schematic 2D representation of the different zones of study.

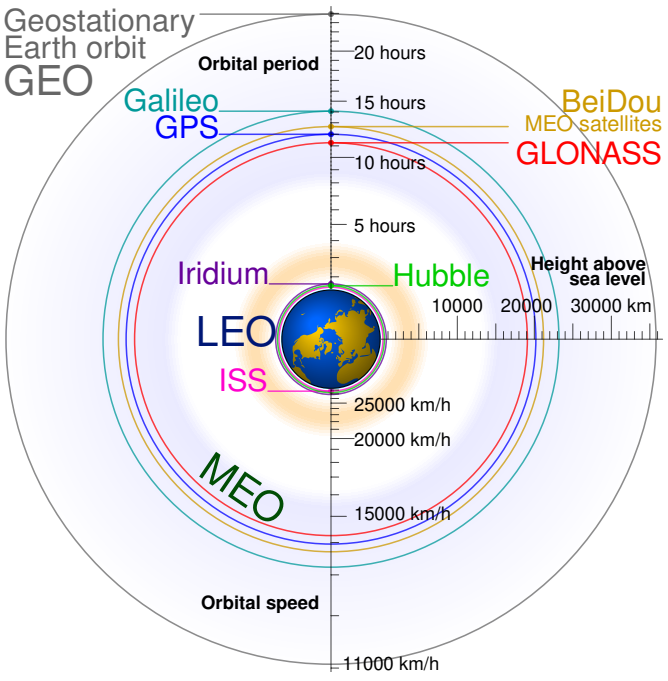

Figure 22: Schematic 2D orbit size comparison of some orbits of satellites used in the simulation. Based on [cmg21].

[10] As mentioned in the introduction, all the code used in this project can be found at https://github.com/victorballester7/final-bachelor-thesis (accessed on June 25, 2023).

[11] The SGP4 model is a mathematical model used to calculate the position of a satellite relative to an Earth-centered inertial coordinated system from the TLE data sets. The SGP4 model was developed by Ken Cranford in 1970. This model was obtained by simplification of the more extensive analytical theory of Lane and Cranford which uses the solution of Brouwer for its gravitational model and a power density function for its atmospheric model. [Mah22]

Along this section we will compare our model with SGP4, instead of with the TLE positions directly. This approach has been considered due to the following reason. We can obtain more easily the positions of the SGP4 propagator model at any instant of time and then compare them with our propagator. Using TLE sets, we can only predict the position at certain fixed times, and that makes the comparison more difficult, specially when the TLEs are very distant in time.

5.2 LEO satellites

We start by simulating the propagation of the trajectories of LEO satellites. We have chosen the *International Space Station* (*ISS*) satellite. Its period is about 90 minutes, so it turns around the Earth about 16 times a day. That affects the propagation of errors, and as LEO satellites interact with the atmosphere and atmospheric drag is difficult to predict, they are the most problematic when it comes to propagating their trajectories. Integrating the system with a duration of 7 days, starting from January 1, 2023, we obtain the following results.

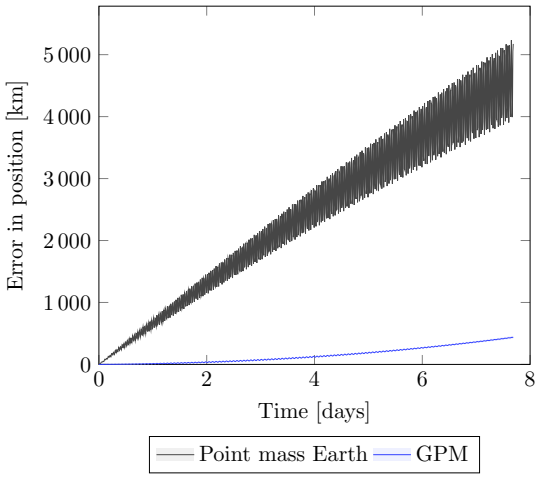

Figure 23: ISS position error when considering the Earth as a point mass or as a non-homogeneous spherical distribution of mass (with the geopotential model).

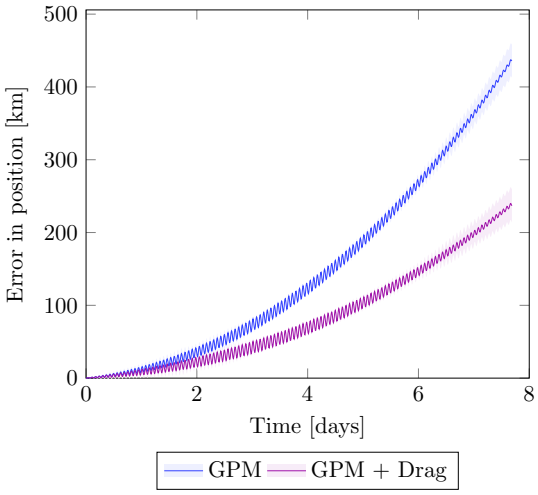

Figure 24: Propagation of the ISS satellite when considering only the geopotential model for the Earth and the atmospheric drag.

Let's make the plots clearer. The left-hand side plot has been made in order to emphasise the improvement in the approximation of the orbit obtained when considering the geopotential model (GPM) with respect to just considering the Earth as a point mass. The right-hand side plot shows two curves, which represent the errors of the position of the ISS (with respect to the SGP4 model) when considering only the geopotential model of the Earth or considering also the atmospheric drag.

In these plots, and all that will follow, each error curve will be within a shaded region in a lighter version of the same color. This shaded region has a vertical width which is equal to twice the linearly interpolated difference between the SGP4 propagation and the real orbit given by TLEs at specific points in time. Its goal is to give the maximum variation that our error curve would have if it was the difference between our propagation and the real orbit, instead of the difference between our propagation and the SGP4 one.

We see that, even not having a precise description of the term $C_{\mathrm{D}}\frac{A}{m}$ in the drag expression, we still decrease notably the error of the position of the satellite when considering the atmospheric drag. During the integration we have assumed a constant value of $C_{\mathrm{D}} = 2.2$, which in basis of [MG05], is reasonable for such conditions, and we have computed the area-to-mass ratio $\frac{A}{m}$ using the mean of the B^* coefficients (see Table 2) of all the TLEs of the ISS and the formula:

$$\frac{A}{m} = \frac{2B^*}{\rho_0 C_{\mathrm{D}}} \tag{117}$$

In this formula, $\rho_0 = 0.157\ \mathrm{kg/(m^2 \cdot R_\oplus)}$ is the reference air density, and $R_\oplus = 6378.1363$ km is the reference Earth radius. The units of B^* in the TLE sets are $1/R_\oplus$.

As the ISS, and other LEO satellites, are far from the Moon and Sun, their influence is negligible for our purposes, and we have not graphically represented them, as their error curves would overlap the purple

curve.

5.3 MEO satellites

As the Harris-Priester model for the density of the atmosphere is not valid for altitudes higher than 1000 km, in MEO satellites, we have not considered it. Instead, the gravitational pull of the Moon and the Sun is considerably high there, namely perturbing the acceleration of the satellite by a factor of 10^{-6} (in SI units), large enough to be considered. The solar radiation pressure is also considered, but we will see that the results are not as good as expected, probably due to the inaccuracy of the model used for it.

This time we have chosen the satellite Sirius-3 and one satellite from the Galileo constellation, namely Galileo-20. The results are shown in Figs. 25 and 26.

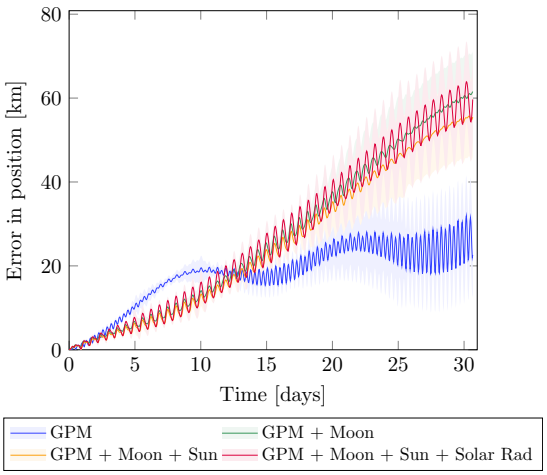

Figure 25: Propagation of the Sirius-3 satellite considering the perturbations from the Moon, the Sun and the solar radiation pressure.

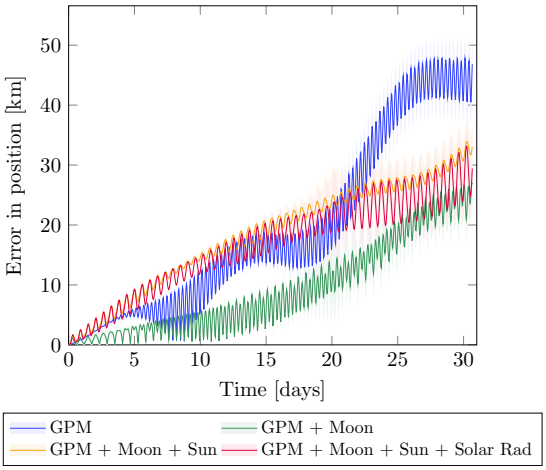

Figure 26: Propagation of the Galileo-20 satellite considering the perturbations from the Moon, the Sun and the solar radiation pressure.

Let's comment the results. First note the change in duration of the integration with respect to the LEO satellites and also the decrease in magnitude of the error. These satellites travel at significantly lower speeds, completing approximately two orbits per day. As a result, the integration time can be much longer and the errors obtained are still comparable. The color codes are the same as the one in the previous plots.

We observe two very distinct results. On the one hand, errors on the Sirius-3 satellite seem to decrease when adding the Sun and Moon into the equations during the first days, although from the beginning of the 12-th day onwards, the blue curve is below the other three, but increasing its oscillations with time.

On the other hand, the situation of the Galileo-20 satellite is very different. The oscillations of the GPM become larger in time and adding the Moon decreases the magnitude of the error but maintains the high oscillation rate. Nevertheless, when enabling the Sun parameter in the equation, the oscillations decrease notably, although the errors in magnitude increase slightly. This could be caused by the fact that the position of the Sun, determined by a deterministic formula given in [MG05], is not accurate enough.

Note that, in both cases, the solar radiation pressure increases the oscillations. Similarly to the atmospheric drag case, we have assumed a constant value of $C_{\mathrm{R}} = 1.55$ (recommended in [MG05]) and a constant ratio $\frac{A_\odot}{m}$ for all the satellites, due to the difficulty on obtaining this data. These imperfections of our model could be having an effect on the simulations.

As a final remark, note that if we consider the point mass approximation for the Earth for MEO spacecraft, the errors obtained are still high, as shown in Fig. 27.

5.4 GEO satellites

Finally, we study the GEO satellite TDRS-3. The results are shown in Fig. 28.

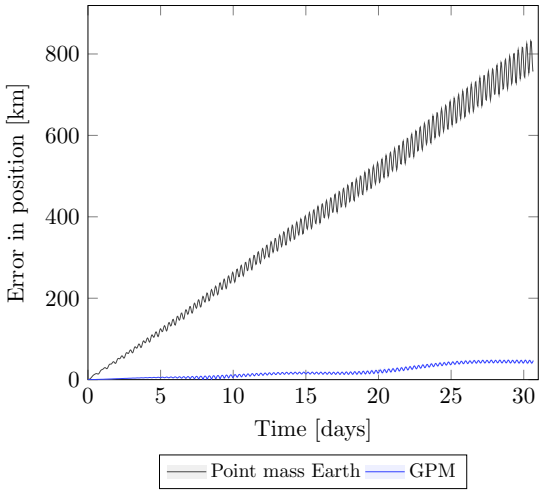

Figure 27: Galileo-20 position error when considering the Earth as a point mass or as a non-homogeneous spherical distribution of mass (with the geopotential model).

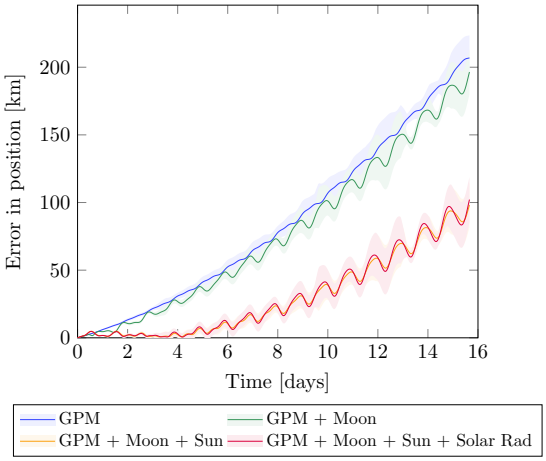

Figure 28: Propagation of the TDRS-3 satellite considering the perturbations from the Moon, the Sun and the solar radiation pressure.

This time, adding the Moon improves only about 10 km of error when comparing it to only using the geopotential model. But adding the Sun really improves the results. In particular, during the first 5 days of integration, the errors with respect to the SPG4 model remain surprisingly small.

It is known (see [MG05]) that geosynchronous satellites require a maneuver approximately each 15 days in order to stay over a specific point above the equator with a tolerance of 0.1 degree in latitude and longitude. The fact that the width of the shaded regions decreases at around the 13th day is compatible with performing a maneuver designed in order to match with its SPG4 propagation. We have no way to check this, but it is reasonable to consider given that the SPG4 propagator is commonly employed in automatic processing to maintain a database of orbiting objects around the Earth.

5.5 General conclusions

On the whole, we have seen how different perturbations affect spacecraft dynamics. In particular, we have observed that the Moon and Sun gravitational attraction become noticeable in MEO an GEO satellites, whereas the atmospheric drag is only important in LEO satellites. In all the cases studied, solar radiation pressure has increased the oscillations of the errors, and therefore, for an extension of this work, it would be interesting to consider more accurate models for solar radiation pressure. The model considered for atmospheric drag is also very simple; considering a more realistic one could also improve the results of this work.

We have not considered the gravitational interaction of other planets, namely Venus, Mars and Jupiter, with the satellites in our simulations. This is because, for our purposes, the influence of other planets on the satellites is negligible due to their large distances from Earth (see [MG05]). In particular, for the date January 1, 2023, which is approximately the initial time of all our integrations, Jupiter was located at a distance of 1.5 AU from Earth. This distance is greater than the distance between the Earth and the Sun, and Jupiter's mass is also much smaller compared to the Sun. Because of that, the gravitational effect of Jupiter is not significant in our simulations, and the same applies to the other planets. In fact, the contribution of all these three planets was of the order of 10^{-11} m/s^2 for MEO satellites, which is negligible when comparing it with the order of magnitude of the perturbations of the Moon and the Sun ($\sim 10^{-6}$ m/s^2).

References

[Ag217] Ag2gaeh. *Elliko-sk*. Mar. 2017. URL: . Accessed: June 04, 2023.

[Aok+81] S. Aoki et al. **?**The new definition of Universal Time.**?** In: *Astronomy and Astrophysics* 105 (Dec. 1981), pp. 359–361.

[Cel] Celestrak. *Celestrak*. URL: . Accessed: June 26, 2023.

[cmg21] cmglee. *Comparison satellite navigation orbits*. Feb. 2021. URL: . Accessed: June 23, 2023.

[Cun70] Leland E. Cunningham. **?**On the computation of the spherical harmonic terms needed during the numerical integration of the orbital motion of an artificial satellite.**?** In: *Celestial mechanics* 2 (Aug. 1970), pp. 207–216.

[Eva10] Lawrence C. Evans. *Partial Differential Equations*. Second Edition. Americal Mathematical Society, 2010. ISBN: 978-0-8218-4974-3.

[GPS02] H. Goldstein, C.P. Poole, and J. Safko. *Classical Mechanics*. Pearson, 2002. ISBN: 978-81-317-5891-5.

[Kel] T.S. Kelso. *Frequently Asked Questions: Two-Line Element Set Format*. URL: . Accessed: April 29, 2023.

[Las07] Lasunncty. *Orbit1*. Oct. 2007. URL: . Accessed: June 04, 2023.

[Lie+77] J. H. Lieske et al. **?**Expressions for the Precession Quantities Based upon the IAU (1976) System of Astronomical Constants.**?** In: *Astronomy and Astrophysics* 58 (June 1977). Provided by the SAO/NASA Astrophysics Data System, pp. 1–16. URL: . Accessed: June 25, 2023.

[Mah22] Meysam Mahooti. *SGP4*. Oct. 2022. URL: . Accessed: June 26, 2023.

[Mat12] Magister Mathematicae. *Conic Sections*. Mar. 2012. URL: . Accessed: April 29, 2023.

[Mez] Hamid Meziani. *Legendre Polynomials and Applications*. URL: . Accessed: April 7, 2023.

[MG05] Oliver Montenbruck and Eberhard Gill. *Satellite Orbits: Models, Methods, and Applications*. Springer, 2005. ISBN: 978-3-540-67280-7.

[Obsa] U.S. Naval Observatory. *IERS Rapid Service / Prediction Center*. URL: . Accessed: April 17, 2023.

[Obsb] U.S. Naval Observatory. *IERS Rapid Service / Prediction Center - Daily Earth Orientation Parameters Solutions*. URL: . Accessed: June 9, 2023.

[RHB99] K.F. Riley, M.P. Hobson, and S.J. Bence. *Mathematical Methods for Physics and Engineering: A Comprehensive Guide*. Cambridge University Press, 1999. ISBN: 978-0-521-86153-3.

[RS98a] International Earth Rotation and Reference Systems Service. *IERS Bulletin A*. July 1998. URL: . Accessed: April 17, 2023.

[RS98b] International Earth Rotation and Reference Systems Service. *IERS Bulletin C*. July 1998. URL: . Accessed: April 17, 2023.

[Spa] Space-track. *Space-track*. URL: . Accessed: June 26, 2023.

[Val13] David A. Vallado. *Fundamentals of Astrodynamics and Applications*. Ed. by Wayne D. McClain. The Space Technology Library, 2013. ISBN: 978-1-881-88318-0.

[VC08] David A. Vallado and Paul Crawford. **?**SGP4 Orbit Determination.**?** In: *AIAA/AAS Astrodynamics Specialist Conference and Exhibit*. 2008. DOI: . URL: . Accessed: June 26, 2023.

[Val+06] David A. Vallado et al. **?**Revisiting Spacetrack Report #3.**?** In: *AIAA/AAS Astrodynamics Specialist Conference and Exhibit*. 2006. DOI: . URL: . Accessed: June 23, 2023.

[Val+] David A. Vallado et al. *Software SGP4*. URL: . Accessed: June 26, 2023.

[Wan+09] Aiping Wang et al. **?**Completeness of Eigenfunctions of Sturm-Liouville Problems with Transmission Conditions.**?** In: *Methods Appl. Anal.* 16 (Sept. 2009). DOI: .

[Wei] Eric W. Weisstein. *Associated Legendre Polynomial. From MathWorld—A Wolfram Web Resource*. URL: . Accessed: April 7, 2023.

[Wika] The Free Encyclopedia Wikipedia. *Earth-centered inertial*. URL: . Accessed: April 14, 2023.

[Wikb] The Free Encyclopedia Wikipedia. *Satellite collision*. URL: . Accessed: June 26, 2023.

[Wikc] The Free Encyclopedia Wikipedia. *Simplified perturbations models*. URL: . Accessed: April 29, 2023.

[Wikd] The Free Encyclopedia Wikipedia. *Sturm-Liouville theory*. URL: . Accessed: April 7, 2023.